

NOTE: The following paper will appear in the 2013 volume of *Annual Reviews of Astronomy and Astrophysics*.

Asteroseismology of Solar-Type and Red-Giant Stars

WILLIAM J. CHAPLIN, ANDREA MIGLIO

*School of Physics and Astronomy, University of Birmingham, Edgbaston,
Birmingham, B15 2TT, UK*

Key Words

stars: oscillations – stars: late-type – stars: solar-type – Galaxy: stellar content
– planet-star interactions

Abstract

We are entering a golden era for stellar physics driven by satellite and telescope observations of unprecedented quality and scope. New insights on stellar evolution and stellar interiors physics are being made possible by asteroseismology, the study of stars by the observation of natural, resonant oscillations. Asteroseismology is proving to be particularly significant for the study of solar-type and red-giant stars. These stars show rich spectra of solar-like oscillations, which are excited and intrinsically damped by turbulence in the outermost layers of the convective envelopes. In this review we discuss the current state of the field, with a particular emphasis on recent advances provided by the *Kepler* and CoRoT space missions and the wider significance to astronomy of the results from asteroseismology, such as stellar populations studies and exoplanet studies.

CONTENTS

Introduction	3
A little background theory: solar-like oscillations	6
Observational data for solar-like oscillators	16
Asteroseismic inference on stellar properties	24
<i>Use of average seismic parameters, and asteroseismic scaling relations</i>	25
Inference from individual oscillation frequencies	32
<i>Estimation of stellar properties</i>	32
<i>Use of signatures of modes of mixed character</i>	35
<i>Use of signatures of abrupt structural variation</i>	39
<i>Inferences on internal rotation</i>	50
Asteroseismology, exoplanets, and stellar activity studies	54
Asteroseismology and stellar populations studies	61
Concluding Remarks	66
Acknowledgements	67

1 Introduction

Almost two decades have passed since a general review of asteroseismology appeared in this journal (Brown & Gilliland 1994, Gautschy & Saio 1995, 1996). At the time, data on solar-like oscillations – pulsations excited and damped by near-surface convection – were available for only one star, the Sun, and the case for detections having been made in other solar-type stars was mixed at best. That situation has since changed dramatically. There are already several ex-

cellent reviews in the literature which discuss the huge efforts and considerable ingenuity that went into detecting oscillations in solar-type and red-giant stars using ground-based telescopes and Doppler-velocity instrumentation (for a detailed overview, see Bedding 2011 and references therein). The concerted drive to reduce noise levels for the detection of exoplanets led to considerable benefits for asteroseismic studies. To results from episodic ground-based campaigns were added a few detections from the first space-based photometric observations of solar-like oscillations (e.g., WIRE, MOST and SMEI; again, see Bedding 2011 and references therein). However, it was the launch of the French-led CoRoT satellite (in late 2006) and the NASA *Kepler* Mission (in 2009) that heralded major breakthroughs for the field: exquisite quality photometric data are now available on solar-like oscillations in unprecedented numbers of solar-type and red-giant stars. *Kepler* has provided multi-year, uninterrupted coverage on many of these targets, with its asteroseismology programme being conducted by the *Kepler* Asteroseismic Science Consortium (KASC; see Kjeldsen et al. 2010, Gilliland et al. 2010).

This review has two overarching themes: first, how data on solar-like oscillations can now test theories of stellar structure, stellar dynamics and evolution, and constrain the physics of stellar interiors, sometimes in ways that have, hitherto, not been possible; and second, how precise estimates of the fundamental properties of stars obtained from asteroseismology impact more widely on astrophysics. We consider two areas in particular that highlight the second theme: the study of the structure, dynamics and evolution of exoplanetary systems, and stellar population and Galactic evolution studies.

Our review is organised as follows. We begin in Section 2 with a concise de-

scription of the key features of solar-like oscillations. We show how the oscillation spectrum changes as the star evolves, in ways that allow us to use seismology to diagnose the stellar properties and internal structure. Section 3 summarizes the observational data that are available from *Kepler* and CoRoT, and some of the key data-analysis challenges. In Section 4, we discuss the use of average or global asteroseismic parameters in estimation of the fundamental stellar properties. Section 5 begins by summarizing key issues for stellar properties estimation when estimates of individual oscillation frequencies are available. We then explain how the individual frequencies may be used to probe the internal structure and dynamics, and test stellar interiors physics. Sections 6 and 7 present the strong links that asteroseismology has with studies of exoplanets, stellar activity and stellar populations. We conclude our review in Section 8 with some remarks on future prospects for asteroseismology.

It is worth stressing that this is currently a very fast-moving field, thanks in large part to the data collected by *Kepler* and CoRoT. Most of the results discussed in the review come from these missions. Our aim is to provide the non-expert with a good overview of recent progress and future opportunities. Many papers have recently been published, and it is not possible to cite them all. We have therefore also tried to cite papers that serve as a useful entry to the subject for those wishing to explore further. Aerts, Christensen-Dalsgaard & Kurtz (2010) provide an excellent overview and introduction to asteroseismology in general. Some recent reviews and articles on asteroseismology of solar-like oscillators include Cunha et al. (2007), Christensen-Dalsgaard & Houdek (2010), Bedding (2011), Christensen-Dalsgaard (2011) and Michel & Baglin (2012).

2 A little background theory: solar-like oscillations

The oscillations have their physical origins in two types of standing waves, those that are predominantly acoustic in character (commonly referred to as pressure modes or p modes) where gradients of pressure act as the restoring force; or internal gravity waves (g modes), where the effects of buoyancy are relevant. Modes of mixed character may also exist, displaying g-mode like behaviour in the central region of a star, and p-mode like behaviour in the envelope.

Solar-like oscillations are intrinsically stable: they are driven stochastically and damped intrinsically by vigorous turbulence in the superficial layers of the sub-surface convection zone (e.g., see Houdek et al. 1999, Samadi & Goupil 2001, and references therein). A necessary condition for stars to show solar-like oscillations is therefore the presence of near-surface convection. The oscillation spectra shown by solar-type and red-giant stars are very rich, with multiple overtones excited to observable amplitudes. Because of geometrical cancellation, only modes of low angular (spherical) degree, l , can be observed.

In this section we shall consider the oscillation spectra of cool stars in different evolutionary states, beginning with main-sequence stars which show spectra of pure p modes. Our purpose is to lay some of the ground work for detailed discussion of results and future prospects in following sections, where we also elaborate on some of the theory (as appropriate). We begin here by using expressions based on an asymptotic treatment to illustrate the principal characteristics of the spectra. The asymptotic formalism has its limitations, particularly when describing the oscillation characteristics of evolved stars. Indeed, significant deviations from asymptotic behaviour can even become apparent in main-sequence stars. We shall see that these deviations may be used to make key inferences on

the internal structures of the stars.

Detectable p modes in main-sequence stars have high overtone numbers (radial orders) n , meaning asymptotic theory may be applied to describe the frequencies ν_{nl} (i.e., as $l/n \rightarrow 0$). An approximate expression given to second order may be written (e.g., see Gough 1986, Christensen-Dalsgaard & Houdek 2010):

$$\nu_{nl} \simeq \Delta\nu \left(n + \frac{l}{2} + \epsilon \right) - \Delta\nu^2 \left[\frac{A[l(l+1)] - B}{\nu_{nl}} \right], \quad (1)$$

where

$$\Delta\nu = \left(2 \int_0^R \frac{dr}{c} \right)^{-1} \quad (2)$$

is the inverse of the acoustic diameter, i.e., the sound travel time across a stellar diameter, c being the sound speed and R the stellar radius, and the coefficient ϵ depends on the cavity boundary conditions, the behaviour close to the stellar surface being most important. The coefficient A in the second-order term is given by

$$A = \left(4\pi^2 \Delta\nu \right)^{-1} \left[\frac{c(R)}{R} - \int_0^R \frac{dc}{dr} \frac{dr}{r} \right], \quad (3)$$

while B is a small correction that also depends on the surface boundary conditions.

The leading term on the right-hand side of Equation 1 implies a dominant overtone spacing in the spectrum, the so-called large frequency separation between modes of the same l , i.e., $\Delta\nu_{nl} = \nu_{nl} - \nu_{n-1l} \simeq \Delta\nu$. Modes of even and odd degree should be separated by $\simeq \Delta\nu/2$. The final term on the right-hand side describes the departure from the degeneracy $\nu_{nl} \approx \nu_{n+1l-2}$ implied by the first term, i.e.,

$$\delta\nu_{l+2}(n) = \nu_{nl} - \nu_{n-1l+2} \simeq -(4l+6) \frac{\Delta\nu}{4\pi^2 \nu_{nl}} \int_0^R \frac{dc}{dr} \frac{dr}{r}. \quad (4)$$

This so-called small frequency separation depends on the sound-speed gradient in the central regions, which in main-sequence stars depends critically on the evolutionary state. In the asymptotic limit, Equation 1 implies that $\delta\nu_{13}(n) = 5/3 \delta\nu_{02}(n)$. Other useful small frequency separations may be formed by $l = 0$ and $l = 1$ modes (e.g., see Roxburgh 2009 and references therein). For example, the small separation $\delta\nu_{01}(n) = \nu_{n0} - \frac{1}{2}(\nu_{n-11} + \nu_{n1})$ measures deviations of $l = 0$ frequencies from the exact halfway frequencies of the adjacent $l = 1$ modes; while $\delta\nu_{10}(n) = \frac{1}{2}(\nu_{n0} + \nu_{n+10}) - \nu_{n1}$ does the same for $l = 1$ frequencies and the adjacent $l = 0$ modes. In the asymptotic limit, $\delta\nu_{01}(n) = \delta\nu_{10}(n) = 1/3 \delta\nu_{02}(n)$. Similar separations may also be formed from combinations of five (or more) frequencies. Frequency separation ratios (Roxburgh & Vorontsov 2003) are formed by taking the ratio of small to large frequency separations, e.g., $r_{02}(n) = \delta\nu_{02}(n)/\Delta\nu_1(n)$. Use of these ratios offers the advantage that they are somewhat insensitive to the structure of the near-surface layers of stars – which are poorly described by models – because the small and large separations are affected in a similar way by near-surface effects. We discuss the issue of the near-surface layers later in Section 5.1. As noted previously, it should be borne in mind that the asymptotic expressions may provide poor descriptions in more evolved stars.

Rotation lifts the degeneracy in the oscillation frequencies ν_{nl} , so that the frequencies of non-radial modes ($l > 0$) depend on the azimuthal order, m . For the fairly modest rates of rotation typical of solar-like oscillators we may ignore, to first order, the effects of the centrifugal distortion. Only in the most rapidly rotating solar-like oscillators are these effects expected to give rise to measureable frequency asymmetries of detectable high- n , low- l p modes (Reese, Lignières & Rieutord

2006; Ballot 2010). The $2l + 1$ rotationally split frequencies may be written:

$$\nu_{nlm} \equiv \nu_{nl} + \delta\nu_{nlm}, \quad (5)$$

with

$$\delta\nu_{nlm} \simeq \frac{m}{2\pi} \int_0^R \int_0^\pi K_{nlm}(r, \theta) \Omega(r, \theta) r \, dr \, d\theta. \quad (6)$$

Here, $\Omega(r, \theta)$ is the position-dependent internal angular velocity (in radius r , and co-latitude θ), and K_{nlm} is a weighting kernel that reflects the sensitivity of the mode to the internal rotation. For the high-order p modes observed in solar-like oscillators, modest rates of differential rotation (in latitude and radius) and absolute rotation mean the splittings $\delta\nu_{nlm}$ of the observable modes will typically take very similar values (hence tending to the approximation of solid-body rotation). The above neglects any contributions to the splittings from near-surface magnetic fields, which give rise to frequency asymmetries of the observed splittings. We might expect to detect departures from symmetry in more active stars (Gough & Thompson 1990), a point we return to briefly in subsequent sections.

Figure 1 shows in detail the observed oscillation spectrum of the G-type main-sequence star 16 Cyg A (KIC 12069424, HD 186408; see Metcalfe et al. 2012), the more massive component of the solar-type binary system 16 Cyg, two of the brightest stars with *Kepler* data. The observed frequencies and frequency splittings carry information on the internal structure and dynamics of the star, and may in turn be used to place tight constraints on the fundamental stellar properties (including the age). As noted previously, the dominant spacing visually is the large frequency separation. The average large separation $\langle \Delta\nu_{nl} \rangle$ is to good approximation equal to $\Delta\nu$ in Equation 1, and hence provides a measure of the acoustic radius of the star. In turn, it may be shown that the average large

separation scales to very good approximation with the square root of the mean density (Ulrich 1986), i.e.,

$$\langle \Delta\nu_{nl} \rangle \propto \langle \rho \rangle^{1/2}, \quad (7)$$

since the frequencies and overtone spacings are related to the dynamical timescale of the star.

The top-left hand panel of Figure 2 shows a so-called échelle diagram of the oscillation spectrum of 16 Cyg A. This was made by dividing the oscillation spectrum into segments of length $\langle \Delta\nu_{nl} \rangle$ in frequency. The segments are then arranged above one another, in order of ascending frequency. Were stars to show a strict correspondence to Equation 1 vertical, straight ridges would be found in the échelle diagram (assuming use of the correct spacing), since the overtone spacings would all be exactly equal to $\Delta\nu$. In practice, stars show departures from this simple description. In main-sequence stars, like 16 Cyg A, those departures are modest but clearly detectable. They carry frequency signatures of regions of abrupt structural change in the stellar interiors, e.g., the near-surface ionization zones and the base of the convective envelope, which we discuss in Section 5.3; and more subtle signatures due to small convective cores (if present; see Section 5.3.2), and the general background state.

It is worth remarking that $l = 3$ modes are detectable in 16 Cyg A. This is due to the exceptional quality of its *Kepler* data. Indeed, the quality is so good that the S/N in the modes is limited by intrinsic stellar noise, and not by shot noise. Typically, CoRoT and *Kepler* give useable data for solar-type stars up to $l = 2$, with the very weak $l = 3$ modes usually lost in the noise (see also Section 3 below).

The oscillation peaks in the frequency-power spectrum have an underlying

Lorentzian-like appearance, i.e., the form expected for damped oscillations. The widths of the Lorentzians provide a measure of the linear damping rates, while the amplitudes – which increase with decreasing $\log g$, as stars evolve – are set by the delicate balance between the excitation and damping. Small asymmetries of the Lorentzian peaks are detectable in solar p modes, and are expected in other stars. These asymmetries arise from the very localized (in radius) excitation source, and the correlation of the p-mode signal and granulation signal (the latter excites and damps the former; e.g., see Roxburgh & Vorontsov 1997). Measurement of the excitation and damping parameters provides the means to infer various important properties of the still poorly understood near-surface convection (e.g., see Chaplin et al. 2005, Samadi et al. 2007, Houdek 2010).

The observed powers of modes in the oscillations spectrum are modulated in frequency by a Gaussian-like envelope (see top left-hand inset of Figure 1). The frequency of maximum oscillations power, ν_{\max} , carries diagnostic information on the excitation and damping and hence physical conditions in the near-surface layers. The behaviour of waves close to the surface is influenced strongly by the acoustic cut-off frequency, ν_{ac} , which is given by

$$\nu_{\text{ac}}^2 = \left(\frac{c}{4\pi H} \right)^2 \left(1 - 2 \frac{dH}{dr} \right), \quad (8)$$

with c the speed of sound and $H = -(\text{d} \ln \rho / \text{d}r)^{-1}$ the density scale height. The sharp rise in ν_{ac} close to the surface of a star describes an efficient boundary for the reflection of waves having $\nu < \nu_{\text{ac}}$, hence fixing a notional upper limit in frequency for the trapped oscillations.

Brown et al. (1991) conjectured that $\nu_{\max} \propto \nu_{\text{ac}}$, since both frequencies are determined by the near-surface properties. We may turn this into a relation linking ν_{\max} to measureable surface properties of a solar-like oscillator by noting

that for the relevant stellar models little accuracy is lost by applying an isothermal approximation of Equation 8, where $\nu_{\text{ac}} = c/(4\pi H)$. This suggests a scaling relation of the form (Kjeldsen & Bedding 1995):

$$\nu_{\text{max}} \propto \nu_{\text{ac}} \propto \frac{c}{H} \propto g T_{\text{eff}}^{-1/2}, \quad (9)$$

where $g \propto M/R^2$ is the surface gravity and T_{eff} is the effective temperature of the star. As a solar-type star evolves, the frequencies shown by its most prominent oscillations will therefore decrease, largely in response to the falling surface gravity. Figure 3 shows the oscillation spectra of five stars observed by *Kepler* (including 16 Cyg A), each having a mass around $1 M_{\odot}$. Surface gravity decreases from top to bottom by about one order of magnitude. The top two stars lie on the main sequence; the third and fourth stars are subgiants, whilst the bottom star lies near the base of the red giant branch (RGB). As we shall see in Section 4.1, Equation 9 appears to work remarkably well in practice, although the power envelopes of some of the hottest F-type stars have a flatter maximum (e.g., Procyon A; see Arentoft et al. 2008) raising question marks over the diagnostic potential, and even the definition or meaning, of ν_{max} in those stars. More work is clearly needed to understand the observed ν_{max} scaling, and theoretical studies have made progress on the problem (e.g., see Belkacem et al. 2011).

After cessation of hydrogen core burning, stars leave the main sequence and their oscillation spectra become more complicated. This is because there is no longer a clear separation of the frequency ranges that will support p modes and g modes. The behaviour is controlled largely by the buoyancy or Brunt-Väisälä frequency, N , given by

$$N^2 = g \left(\frac{1}{\Gamma_1} \frac{d \ln p}{dr} - \frac{d \ln \rho}{dr} \right). \quad (10)$$

The g modes have frequencies that are lower than N , and high-order g modes may be described by an asymptotic relation in the periods, Π_{nl} , i.e.,

$$\Pi_{nl} = \nu_{nl}^{-1} \simeq \Delta\Pi_l (n + \epsilon_g), \quad (11)$$

where the period separation $\Delta\Pi_l$ (analogous to $\Delta\nu$ for p modes) is given by:

$$\Delta\Pi_l = \frac{2\pi^2}{\sqrt{l(l+1)}} \left(\int_{r_1}^{r_2} N \frac{dr}{r} \right)^{-1}, \quad (12)$$

assuming that $N^2 \geq 0$ in the convectively stable region bounded by $[r_1, r_2]$, with $N = 0$ at r_1 and r_2 (Tassoul 1980).

After exhaustion of the central hydrogen, the buoyancy frequency in the deep stellar interior increases to such an extent that it extends into the frequency range of the high-order p modes. When the frequency of a g mode comes close to that of a non-radial p mode of the same degree, l , the modes undergo an “avoided crossing” (Aizenman, Smeyers & Weigert 1977), which is analogous to avoided crossings of atomic energy states. Interactions between the modes will affect (or bump) the frequencies and also change the intrinsic properties of the modes, so that they take on mixed p and g characteristics (having a g-mode character in the deep interior and a p-mode character in the envelope).

The first subgiant showing evidence of an avoided crossing in its oscillation spectrum (η Boo) also happened to be the first case of a star other than the Sun showing unambiguous evidence of solar-like oscillations (Kjeldsen et al. 1995, Christensen-Dalsgaard, Bedding & Kjeldsen 1995). Ground-based observations also provided another case of a subgiant showing mixed modes (β Hyi; see Bedding et al. 2007). *Kepler* and CoRoT have now added a significant number of further cases, with much more precisely determined oscillation frequencies. The top right-hand panel of Figure 2 shows the échelle diagram of one such *Kepler* target, the G-type

subgiant KIC 6442183 (HD 183159; see also Figure 3). First, we note that the $l = 0$ p modes are unaffected by the phenomenon because perturbations in buoyancy will not support radial modes, and so there are no g modes for the radial p modes to couple to. However, several $l = 1$ p modes have been significantly shifted from the putative, undisturbed $l = 1$ ridge (including one mode that has been shifted close to the $l = 0$ ridge). The larger the shift in frequency from the undisturbed ridge, the stronger is the interaction or coupling between the p and g modes. The coupling is much weaker at $l = 2$.

The frequency of the avoided crossing – where the frequency perturbation changes sign, across the undisturbed ridge – corresponds to the pure g-mode frequency that the star would show if it was comprised only of the central, g-mode cavity, and is hence a sensitive diagnostic of the core properties and the exact evolutionary state of the star. The displaced $l = 1$ frequencies of KIC 6442183 are examples of several p modes coupling to a single g mode. The detectability of the modes may be partially understood in terms of the mode inertia, a measure of the fraction of the star’s mass that is engaged in pulsation (e.g., see Aerts, Christensen-Dalsgaard & Kurtz 2010). The g-dominated mixed modes have high mode inertias because their eigenfunctions show large amplitudes in the core, where the density is high; this contributes to making them undetectable in the observations (see also Section 3 below). The amplitudes of the eigenfunctions of the p-dominated modes are in contrast highest in the envelope, hence these modes are clearly detectable.

The impact of mode coupling is much more apparent in red giants, leading to a much richer ensemble of observable signatures (Dupret et al. 2009), which, as we shall see in later sections, may be used to discriminate different advanced

phases of evolution. Figure 4 shows the oscillation spectra of four red giant stars observed by *Kepler*, again all having masses around $1 M_{\odot}$. The middle panel of Figure 2 shows the échelle diagram of one of these stars, KIC 6949816, a star ascending the RGB. The observed oscillation frequencies are significantly lower than in earlier phases of evolution. Again, this is largely the result of the marked expansion of the outer layers in the post main-sequence phase, which leads to a large reduction in the surface gravity.

In the main-sequence phase we see one $l = 1$ mode in each radial order. In the early post main-sequence phase it may be possible to observe more than one $l = 1$ mode per order, assuming the g-dominated modes have a low enough inertia to be detectable. In the red-giant phase there is a much denser spectrum of g modes for the p modes to couple to, so that there are potentially many observable $l = 1$ mixed-modes per order, as is apparent from Figure 2 (middle panel) and Figure 4 (top panel, notably at frequencies around 77 and 85 μHz). The p-dominated mixed modes are most likely to be observed (again, because they have lower inertia than their g-dominated counterparts). Here, at each order we see a cluster of p-dominated mixed modes, arranged about the putative, undisturbed pure p-mode frequency at that order. Because the observed mixed modes are not pure g modes, the observed period spacings are in practice smaller than those implied by Equation 12.

Following ignition of helium (He) in the core, stars enter a relatively long-lived core-He burning phase. The ignition of He in low mass stars takes place in a highly degenerate He core of mass $\approx 0.47 M_{\odot}$, irrespective of the total mass of the star. This He flash is followed by a structural readjustment resulting in an accumulation of stars in the Hertzsprung-Russell diagram known as the Red

Clump (RC). The bottom right-hand panel of Figure 2 shows the échelle diagram of an RC star, KIC 7522297 (see also Figure 4). Its oscillation spectrum is very complicated, in contrast to the spectrum of KIC 3100193 (bottom left-hand panel, and again Figure 4), an RGB star with similar surface properties and hence a similar ν_{\max} . In Section 5.2 we shall discuss at some length use of the g-mode period spacings as a diagnostic of the evolutionary state, and see that increased period spacings in RC stars allows them to be distinguished from RGB stars that lie in close proximity in the Hertzsprung-Russell diagram.

3 Observational data for solar-like oscillators

Asteroseismology is currently an observationally driven field, with large volumes of exquisite quality long timeseries data now available, in particular from *Kepler* and CoRoT. Their long datasets give the frequency resolution needed to extract accurate and precise estimates of the basic parameters of individual modes covering several radial orders, such as frequencies, frequency splittings, amplitudes, and damping rates. Uninterrupted data offer huge advantages for the analysis. The diurnal gaps present in ground-based observations cause well-known frequency-aliasing problems. The frequency separations associated with the resulting “sidebands” can be close to the characteristic frequency separations presented by solar-like oscillators, making interpretation of the observed spectra more difficult. A less well-known problem arises from the fact that ground-based window functions typically also carry a quasi-random component (e.g., weather), which introduces quasi-white (i.e., broadband) noise in frequency. This may significantly degrade the underlying signal-to-noise ratio in the modes.

In spite of these complications, ground-based Doppler velocity observations

have an important rôle to play. The signatures of granulation are much less prominent in velocity, relative to the oscillations, than they are in photometry. Since the amplitude of the granulation signal increases with decreasing frequency (i.e., its spectrum is “pink”), the intrinsic stellar noise presents less of a challenge to the detectability of low-frequency modes when observations are made in velocity. In main-sequence stars, these modes present the narrowest widths in frequency (being more lightly damped than their higher-frequency counterparts) and so it is possible to extract extremely accurate and exquisitely precise frequencies and rotational frequency splittings for making inference on the internal structure and dynamics. Doppler velocity observations are also more sensitive to modes of $l = 2$ and 3 than are photometric observations. Finally, when complementary photometric and Doppler-velocity data are available on the same target, important inferences can be made on the interactions of the oscillations with the convection, and the physics of non-adiabatic processes in the near-surface layers of the star (Houdek et al. 1999, Houdek 2010, Huber et al. 2011a). Results of such comparisons can help to calibrate convection models and the treatment of radiative transport.

Asteroseismic detections provided by *Kepler* and CoRoT are considerably more numerous for red giants than for solar-type stars. Detection of oscillations in solar-type stars requires the target-limited, short-cadence data¹ of each mission (58.85 s and 32 s cadences, respectively) since the dominant oscillations have periods of the order of minutes. These short periods are not accessible to the long-cadence data of either mission (having 29.4 min and 8.5 min cadences, re-

¹CoRoT had the capability to observe up to 10 targets simultaneously in short cadence, and five following the failure of one of its detectors. *Kepler* has the capability to observe up to 512 targets simultaneously in short cadence.

spectively). The periods and amplitudes of the oscillations in red giants are significantly longer and higher, respectively – the strongest oscillations of stars at the base of the RGB having periods of the order of 1 hr – meaning oscillations may be detected in fainter (more numerous) targets observed in long cadence.

CoRoT provided the first multi-month datasets on solar-type stars (Michel et al. 2008) and red giants (De Ridder et al. 2009). At the time of writing the short-cadence “seismo” observations have provided asteroseismic datasets on 12 solar-type stars in the apparent magnitude range $5.4 \leq m_v \leq 9.4$, with dataset lengths ranging from 20 to 170 days. The long-cadence “exo” observations have yielded asteroseismic datasets of similar length on more than one thousand red giants in the range from roughly $11 \lesssim m_v \lesssim 16.5$ (e.g. Hekker et al. 2009, Mosser et al. 2011b), and in several different fields (as we shall discuss later in Section 7). There had previously been some debate as to whether red giants would show detectable non-radial modes, but CoRoT resolved the issue with unambiguous detections in many targets.

Kepler has revolutionized asteroseismology of solar-type stars. During the first 10 months of science operations an asteroseismic survey yielded detections of solar-like oscillations in more than 500 stars observed for one month each in short cadence (Chaplin et al. 2010, 2011). These data span spectral types from early F through to late K, with most targets in the *Kepler* apparent magnitude range $8 \leq K_p \leq 12$. There are a small number of even brighter targets, for which special dedicated photometry masks have been designed. These include the brightest star falling on detector pixels, the F-type star θ Cyg, and the G-type binary comprised of the solar-analogues 16 Cyg A and B (Metcalf et al. 2012). These data represent a unique, homogeneous ensemble for testing stellar evolutionary theory.

Around 150 solar-type stars with the highest-quality data were subsequently selected to be observed for longer durations in short cadence. These stars now have data ranging in length from several months to years. Around 60 stars should be observed for the entire duration of the mission.

The long-cadence *Kepler* data have yielded asteroseismic data of unprecedented quality on stars in the red-giant phase (e.g., see Bedding et al. 2010, Huber et al. 2010, Kallinger et al. 2010, Hekker et al. 2011b), including giants in the open clusters NGC 6791, NGC 6819 and NGC 6811 (Stello et al. 2011b; the clusters are most likely too faint to allow detection of oscillations in solar-type stars). High-quality asteroseismic data are available on around 14,000 red giants having uninterrupted coverage throughout the first 3.5 yr of the mission. The expectation is that many of these targets will have continued observations throughout the extended mission. These very long datasets will be required to yield accurate seismic information on stars near the tip of the RGB, and on the asymptotic giant branch (AGB) where ν_{\max} and $\langle\Delta\nu_{nl}\rangle$ are both small fractions of a μHz in size.

We come back in Section 6 to the approximately 80 *Kepler* asteroseismic targets that are also confirmed, validated or candidate exoplanet host stars.

Figure 5 summarizes the asteroseismic data in-hand on solar-like oscillators, plotting stars with detections on a Hertzsprung-Russell diagram.

Developments in the analysis for CoRoT and *Kepler* have built naturally on the heritage and experience from two areas of the discipline. The analysis of ground-based data on solar-like oscillators offered considerable prior expertise in dealing with moderate quality, low S/N data. This provided the springboard for many of the codes developed to extract average or global properties of the oscil-

lations spectra. The analysis of Sun-as-a-star helioseismology data was another obvious starting point from which to develop techniques for application to main-sequence stars, most notably for modelling and fitting asteroseismic parameters of individual modes.

In preparation for *Kepler*, and the expected large numbers of asteroseismic targets, considerable effort was devoted to developing and testing codes for automated detection of signatures of solar-like oscillations (Verner et al. 2011, Hekker et al. 2011a and references therein), and subsequent extraction of average asteroseismic parameters such as $\langle \Delta\nu_{nl} \rangle$ and the frequency of maximum oscillations power, ν_{\max} (e.g., with hare-and-hounds exercises using realistic, artificial asteroseismic data; see Stello et al. 2009). The much more difficult task of extracting accurate estimates of parameters of individual modes is colloquially referred to as “peak bagging” (e.g., see Appourchaux 2011). Peak-bagging often proceeds by fitting multi-parameter models to the observed oscillation spectra, with the basic building-block being a Lorentzian-like function to describe each resonant peak having an underlying maximum power spectral density or height H and width Γ , where $H \propto A^2/\Gamma$, A being the oscillation amplitude of the mode. In order to resolve the Lorentzian, the length of the timeseries, T , must span several amplitude e-folding lifetimes, τ , where $\Gamma = 1/(\pi\tau)$. The requirement $T/\tau \geq 10$ is a good guideline threshold. When T drops to only 2τ , so the observed profile tends to a sinc-squared function (set by T), and a Lorentzian is no longer the correct function to fit. Indeed, when $T \leq 2\tau$, a sine-wave fitting approach (sometimes, slightly misleadingly, called “pre-whitening”) is the better option (i.e., one then also makes use of the phase information).

Typical peak widths, Γ , in main-sequence stars are of the order of one to

a few μHz , which suggests that observations spanning a month or so will just adequately resolve the peaks. There is however the added complexity of rotation (and magnetic fields). The resulting frequency splittings between adjacent non-radial mode components can range from a fraction to several μHz . In practice, multi-month datasets are required to get good constraints on the peak widths and heights of radial modes in main-sequence stars although it is safe to fit Lorentzian-like models to shorter datasets; while datasets of a year to several years are needed to also fully disentangle and so extract robust rotational splittings (of which more in Section 6), or asymmetries of those splittings resulting from the near-surface magnetic fields.

Lessons learned from CoRoT's first solar-type targets, which were all F-type stars, proved vital to the development of peak-bagging methodology (Appourchaux et al. 2008). The oscillation peaks in these F stars turned out to be very wide in frequency (suggesting very heavy damping of the oscillations) and modes adjacent in frequency were extremely hard to resolve. This presented challenges not only to the fitting but also, crucially, rendered visual inspection of the spectrum useless as a means of tagging correctly the odd and even angular-degree ridges (a problem that now appears to have been solved by using the parameter ϵ from Equation 1 as a diagnostic for identifying the even-degree ridge; see White et al. 2012).

The main lesson learned from CoRoT was that spectra of solar-type stars were not always as straightforward to analyse as the Sun. Further coordinated development and testing of peak-bagging codes, and application to the more numerous *Kepler* stars, has meant that near automation of the peak-bagging is now possible for main-sequence stars and also subgiants that have not yet evolved suf-

ficiently to show many modes of mixed character (see Appourchaux et al. 2012, and references therein). The initial step in the automated fitting packages is to identify modes in the frequency power spectrum from which a robust list of first-guess parameters then follows. Identification often involves statistical testing, using false-alarm or odds-ratio approaches (the latter involving the adoption of priors on the expected mode signal; see Appourchaux 2011). Application of prior information to maximum-likelihood estimation is now also common in peak-bagging, although this must be used with care; and use of Markov Chain Monte Carlo (MCMC) methods is also very fashionable, as in many other areas of astronomy (Gruberbauer et al. 2009, Benomar, Appourchaux & Baudin 2009, Handberg & Campante 2011). While computationally expensive, MCMC offers robust estimation of the posterior distributions (and hence the confidence intervals) of the best-fitting parameters. When the fitting is straightforward (high S/N, with well-constrained fitting distributions) maximum-likelihood estimators offer a more than adequate approach.

As stars evolve through the subgiant phase onto the RGB, the appearance of modes of mixed p and g character offers new challenges, and opportunities, for the fitting. The inertia and through it the damping of the modes is affected by the coupling, so that the observed linewidth Γ of a mixed mode will be reduced by the ratio of the (increased) inertia of the mixed mode and the inertia that a radial mode would have at the same frequency. Provided the modes are well resolved (see above), the mode height will *not* be affected by the coupling. However, when the mode peak is not resolved, the height H will be reduced by the same factor as Γ . The g-dominated modes, which have very high inertia and hence very narrow peak linewidths, are therefore much harder to detect than p-dominated

modes of lower inertia. Those lower-inertia modes that are observable will still have the benefit of presenting narrower linewidths than pure p modes at similar frequencies, helping estimation of frequencies and frequency splittings (as we shall see in Section 5.4).

The complicated spectra found in evolved solar-like oscillators makes extraction of robust lists of identified modes and first-guess parameters non-trivial, although enough is known already about the pathology of the observed spectra to provide useful guidance (e.g., see Huber et al. 2010, Mosser et al. 2011b). Frequency spacings between modes and frequency splittings due to rotation may be very similar, making it hard to disentangle the observed signatures. Use of reasonably strong priors is advisable when fitting. As we learn more about how to handle evolved solar-like oscillators it should be possible to ease these strong priors which in the short-term are probably needed to extract usable frequencies.

Besides the frequencies and frequency splittings, other important data products given by analysis of the oscillation spectra are mode powers and linewidths. The long timeseries of *Kepler* and CoRoT are important for in principle providing unbiased estimates of both parameters. Initial results have been obtained from peak-bagging (e.g., Baudin et al. 2011, Appourchaux et al. 2012) and from other techniques (Huber et al. 2011b, Mosser et al. 2012a) developed from ground-based analysis methods (e.g., Kjeldsen et al. 2008), including results on stars in open clusters (Stello et al. 2011a) and first theoretical interpretation of the results (Belkacem et al. 2012, Samadi et al. 2012).

4 Asteroseismic inference on stellar properties

There is growing effort being devoted to the testing and development of asteroseismic techniques for estimating fundamental stellar properties. These techniques are now making it possible to estimate precise and accurate properties of large numbers of field stars, on which sparse inferences were only previously available.

The most accurate, and precise, stellar properties have come from observations of stars in detached eclipsing binaries (Torres, Andersen & Giménez 2010). Other types of data on bright stars, e.g., trigonometric parallaxes, or interferometric radii, have also provided precise and accurate (largely model-independent) properties. As we shall see later, when asteroseismic observations are also available on these stars it is possible to test the robustness of the asteroseismic techniques. Moreover, excellent prior constraints on the stellar properties allows asteroseismology to make unique tests of stellar interiors physics, something we return to in later sections. The excellent accuracy and precision achievable in asteroseismic estimates of surface gravities is of considerable interest for helping to calibrate spectroscopic data-reduction pipelines, in particular automated pipelines for large-scale surveys (of which more later in Sections 6 and 8).

For many field stars we do not have the luxury of very accurate data on fundamental properties. Stellar properties estimation has then usually had to rely upon the use of spectroscopic or photometric observations of basic surface properties, e.g., colours, gravities and metallicities. Moreover, some uncertainty remains over the solar photospheric composition (Basu & Antia 2008, Asplund et al. 2009), which impacts on the determination of absolute abundances in other stars.

Comparison of these observations with modelled observable surface properties from stellar atmospheres and stellar evolution theory yields “best-fitting”

estimates of the fundamental properties. Such data may provide little, if any, discrimination between stars with different fundamental properties that share similar surface properties. However, the asteroseismic observables – most notably the individual frequencies, which can already be measured to a precision of better than 1 part in 10^4 with *Kepler* data – provide the means to discriminate in such cases. It is important to stress that complementary, non-seismic inputs are required to optimize the potential of the seismic data. At the very least one requires the effective temperature, T_{eff} , to obtain tight constraints on the stellar radius and surface gravity; while in order to fully constrain the mass and age, strong prior constraints on the metallicity are essential (Brown et al. 1994, Basu et al. 2012).

Later, we shall discuss the use of individual frequencies in stellar properties estimation. But first, we shall look at the use of average or global asteroseismic parameters, including application of the asteroseismic scaling relations from Section 2.

4.1 Use of average seismic parameters, and asteroseismic scaling relations

When the S/N ratios in the asteroseismic data are insufficient to allow robust fitting of individual mode frequencies, it is still possible to extract average or global asteroseismic parameters. Indeed, as noted previously, the automated analysis codes developed for application to *Kepler* and CoRoT data have enabled efficient extraction of these parameters on large numbers of stars. The main parameters are the average frequency separation $\langle \Delta\nu_{nl} \rangle$, and the frequency of maximum oscillations power, ν_{max} . It may also be possible to extract the average

small frequency separations (see Section 2) from moderate-quality data.

Equations 7 and 9 imply that if estimates of $\langle \Delta\nu_{nl} \rangle$ and ν_{\max} are available, together with an independent estimate of T_{eff} , “direct” estimation of the stellar radius, mass, mean density and surface gravity is possible. This so-called direct method is particularly attractive because it in principle provides estimates that are independent of stellar evolutionary theory.

The most convenient practical application invokes the assumption that for all evolutionary phases, from the main sequence to the red-giant phase, it is safe to scale against precisely measured solar values of the parameters. Re-arrangement of the scaling relation equations then gives, for example:

$$\left(\frac{R}{R_{\odot}} \right) \simeq \left(\frac{\nu_{\max}}{\nu_{\max,\odot}} \right) \left(\frac{\langle \Delta\nu_{nl} \rangle}{\langle \Delta\nu_{nl} \rangle_{\odot}} \right)^{-2} \left(\frac{T_{\text{eff}}}{T_{\text{eff},\odot}} \right)^{0.5}, \quad (13)$$

$$\left(\frac{M}{M_{\odot}} \right) \simeq \left(\frac{\nu_{\max}}{\nu_{\max,\odot}} \right)^3 \left(\frac{\langle \Delta\nu_{nl} \rangle}{\langle \Delta\nu_{nl} \rangle_{\odot}} \right)^{-4} \left(\frac{T_{\text{eff}}}{T_{\text{eff},\odot}} \right)^{1.5}, \quad (14)$$

$$\left(\frac{\rho}{\rho_{\odot}} \right) \simeq \left(\frac{\langle \Delta\nu_{nl} \rangle}{\langle \Delta\nu_{nl} \rangle_{\odot}} \right)^2 \quad (15)$$

and

$$\left(\frac{g}{g_{\odot}} \right) \simeq \left(\frac{\nu_{\max}}{\nu_{\max,\odot}} \right) \left(\frac{T_{\text{eff}}}{T_{\text{eff},\odot}} \right)^{0.5}. \quad (16)$$

Notice that the form of Equations 13 and 14 imply that estimated masses are inherently more uncertain than radii.

One may also use $\langle \Delta\nu_{nl} \rangle$, in addition to ν_{\max} , as input to so-called “grid-based” estimation of the stellar properties (e.g., Stello et al. 2009, Basu, Chaplin & Elsworth 2010, Quirion, Christensen-Dalsgaard & Arentoft 2010, Gai et al. 2011). This is essentially the well-used approach of matching the observations to stellar evolutionary tracks, but with the powerful diagnostic information contained in the seismic $\langle \Delta\nu_{nl} \rangle$ and ν_{\max} also brought to bear. Properties of stars are determined by searching among a grid of stellar evolutionary models to get a “best match”

to the observed set of input parameters, which should include T_{eff} and $[\text{Fe}/\text{H}]$. While the direct method assumes that all values of temperature are possible for a star of a given mass and radius, we know from stellar evolution theory that only a narrow range of T_{eff} is allowed for a given M and R , assuming a known chemical composition and given stellar interiors physics. This prior information is implicit in the grid-based approach, and means that estimated uncertainties are typically lower than for the direct method because a narrower range of outcomes is permitted. The model grids must be well sampled in the various input parameters. Bazot, Bourguignon & Christensen-Dalsgaard (2012) have recently discussed how use of MCMC techniques may help to mitigate problems related to grid-sampling.

There is one more level of subtlety to consider in application of the grid-based technique. It may rely wholly on the scaling relations, so that the fundamental properties of the models (i.e., R , M , T_{eff}) are used as inputs to compute values of $\langle\Delta\nu_{nl}\rangle$ and ν_{max} for comparison with the observations. Or one may instead compute theoretical oscillation frequencies of each model, and from those compute a suitable average $\langle\Delta\nu_{nl}\rangle$ for comparison with the observations. Another approach to testing the accuracy of the scaling relation for $\langle\Delta\nu_{nl}\rangle$ is therefore to compare the average $\langle\Delta\nu_{nl}\rangle$ implied by the M and R of each model with the average $\langle\Delta\nu_{nl}\rangle$ of the model's computed oscillation frequencies. Comparisons of this type (e.g., Ulrich 1986, White et al. 2011) suggest that for the solar-type stars and RGB stars the relation is accurate to 2 to 3%. Similar comparisons between models of red giants in different evolutionary states show that relative differences in the $\langle\Delta\nu_{nl}\rangle$ scaling of the order few per cent are expected between low-mass stars on the RGB and in the core-helium burning RC phase (Miglio et al. 2012). This

is because low-mass stars with same M and R can have significantly different sound speed profiles, and hence different acoustic radii, in these two evolutionary states. Mosser et al. (2013) have studied the impact of including higher-order terms from asymptotic expressions describing the frequencies (e.g., Equation 1), to estimate modified average large separations for use with the scaling relations.

It is important to note that such comparisons of $\langle \Delta\nu_{nl} \rangle$ do not allow for the impact of poor modelling of the near-surface layers and the effects of this on the model-predicted values of the frequencies, and hence the average large separations. At least in so far as the Sun is concerned, the effect on $\langle \Delta\nu_{nl} \rangle$ is relatively small. However, the issue is much more of a concern when it comes to modelling of the individual frequencies. We shall discuss these surface effects in more detail in Section 5.1 below. Because we have much less confidence in theoretical computations of ν_{\max} – which rely on the complicated excitation and damping processes – than we do in theoretical predictions of the oscillation frequencies, model-computed ν_{\max} have so far not been used in stellar properties estimation. Irrespective, it is clear that much more work is needed to understand the diagnostic potential of ν_{\max} , and how far it can be pushed in terms of accuracy (in particular for high-precision data).

When a grid-based approach is used, accuracy is of course demanded of the stellar evolutionary models. Those models must include all of the requisite physics that we consider to be significant in determining the evolutionary state of the star, and as a result its observable properties. Extensive tests made using a variety of different stellar evolutionary codes have shown that density, surface gravity and radius (and through that luminosity) are largely model independent, and quite insensitive to the input physics (see Lebreton et al. 2008; Monteiro 2009

and references therein). However, the masses and ages are much more sensitive to choices made in construction of the grid of stellar models, in particular the chemical composition, and can be affected by, for example, the inclusion of the effects of microscopic diffusion in the stellar evolutionary models. Overshoot at convective boundaries can also be an issue in this regard. An obvious way to capture the uncertainties in known modelling ingredients is to use a variety of model grids, with different input physics, and then include the resulting grid-to-grid scatter of the estimated properties in the final, quoted uncertainties. This approach has been adopted in the analysis of *Kepler* stars (e.g., on the exoplanet host stars discussed in Section 6). Although, as noted above, the uncertainties on the direct-method estimates are larger than for the grid-based method, one might hope that they are expected to largely capture any uncertainties or systematics in the scaling relations due to, for example, metallicity effects.

How accurate are the scaling relations? Crucial to making fundamental tests of the scaling relations is having independent and accurate estimates of the stellar properties against which to compare the asteroseismic values, on as wide a range of evolutionary states as possible. Tests against independent mass estimates are limited to cases of visual binaries, eclipsing binaries, high S/N exoplanet transits, and to some extent stars in clusters. To test radii it suffices to have accurate parallaxes, and interferometrically measured angular radii.

Bruntt et al. (2010), Bedding (2011) and Miglio (2012) compared asteroseismic and independently determined properties (e.g., from binaries) of a selection of bright solar-type stars and red giants, which all showed solar-like oscillations in observations made from either ground-based telescopes or CoRoT. The estimated properties were found to agree at the level of precision of the uncertainties, i.e.,

to 10% or better. The fundamental comparisons have recently been extended to slightly fainter stars observed by *Kepler*. Silva Aguirre et al. (2012) used asteroseismic data on 22 of the brightest *Kepler* targets with detected solar-like oscillations, and found excellent agreement between stellar radii inferred from the scaling relations and those inferred from using Hipparcos parallaxes (at the level of a few percent). Huber et al. (2012) combined interferometric observations of some of the brightest *Kepler* and CoRoT targets with Hipparcos parallaxes, and also found excellent agreement with the scaling-relation inferred stellar radii, at the 5% level.

The analysis of high S/N exoplanet lightcurves provides accurate and precise stellar densities independent of stellar evolutionary theory, assuming the orbit is well constrained. Four such examples, where solar-like oscillations were also detected in the host star, are TrES-2, HAT-P-7 and HAT-P-11 (Christensen-Dalsgaard et al. 2010), and HD 17156 (Gilliland et al. 2011) (see Section 6). As noted by Southworth (2011) the asteroseismic densities are in good agreement with the lightcurve-derived densities for TrES-2 and HD 17156, but not for HAT-P-7 and HAT-P-11. The prospects for expanding this very small sample look promising, given the healthy yield of asteroseismic exoplanet host stars detected by *Kepler*.

The detection by *Kepler* of solar-like oscillations in red giant members of open clusters has provided additional data for testing the accuracy of the scaling relations, particularly when largely model-independent constraints are available for the cluster members. Independent radius estimates of stars in NGC 6791 based on the distance determination by Brogaard et al. (2011) were used by Miglio et al. (2012) to check the consistency of masses estimated from the scaling relations (Equations 13 and 14). While no significant systematic effect was found on the

RGB, Miglio et al. (2012) suggested that a relative correction to the $\langle \Delta\nu_{nl} \rangle$ scaling relation should be considered between RC and RGB stars (as noted above). If scaling relations are used, this could affect the mass determination of clump stars at the $\sim 10\%$ level. By combining constraints from near-turnoff eclipsing binaries and stellar models, Brogaard et al. (2012) estimated masses of stars on the lower part of the RGB in NGC 6791. Basu et al. (2011) used asteroseismic techniques to estimate an average RGB mass that agreed with Brogaard et al. (2012) to within $\simeq 7\%$. The difference is however significant given the quoted uncertainties, and further work is needed to understand the origin of the discrepancy. Finally, asteroseismic masses of giants in NGC 6819 (Basu et al. 2011, Miglio et al. 2012) are in good agreement (at the $\simeq 10\%$ level) with estimates given by isochrone fitting (Kalirai & Tosi 2004, Hole et al. 2009). It should however be borne in mind that uncertainties and model-dependences associated with the isochrone method mean the resulting data do not provide stringest tests of the asteroseismic masses. Results are however now coming available on eclipsing binaries in NGC 6819, which will allow tighter constraints to be placed on the systematics (as discussed by Sandquist et al. 2013).

Additional and more stringent tests of the asteroseismic scaling relations will be possible in the near future using results from *Kepler* and CoRoT on solar-like oscillators that are members of visual binaries and/or detached eclipsing binaries (e.g., Hekker et al. 2010).

5 Inference from individual oscillation frequencies

5.1 Estimation of stellar properties

Use of individual frequencies increases the information content provided by the seismic data for making inference on the stellar properties. It is therefore possible to tighten constraints on those properties, most notably constraints on the age. Asteroseismology not only provides excellent precision in the age estimates – with realistic levels of 10 to 15% achievable (e.g., see discussions in Lebreton & Montalbán 2009, 2010, Soderblom 2010) – but may also be used to improve the accuracy of the age determinations through tests of stellar models for systems with already well-constrained properties.

The analysis again proceeds via a grid-based approach through comparison of the observed frequencies with frequencies calculated for the grid of stellar evolutionary models, with minimization of the deviations between the observed and modelled parameters yielding the best-fitting solutions.

A well-known problem in comparing observed and model-calculated frequencies comes from the hard-to-model near-surface layers of stars. Models usually employ simplified model atmospheres, and mixing length theory is used to describe convection which leads to errors in the structure of the superadiabatic region. Moreover, model oscillation frequencies calculated in the usual adiabatic approximation neglect the effects of turbulent pressure. In the case of the Sun, this has all been shown to lead to an offset (sometimes called the “surface term”) between observed p-mode frequencies and the model-predicted p-mode frequencies (e.g., see Christensen-Dalsgaard & Thompson 1997, and references therein), with the model frequencies being on average too high by a few μHz (giving a

negative surface term). The offset is larger in modes at higher frequencies (i.e., the closer ν_{nl} is to ν_{ac} ; the lowest-frequency modes are evanescent very close to the surface). As noted previously the average large frequency separation is also affected by the surface term, by an amount that depends on the gradient of the offset with radial order, n . In the case of the Sun, the model-predicted $\langle \Delta\nu_{nl} \rangle$ is about $1 \mu\text{Hz}$ higher than the observed $\langle \Delta\nu_{nl} \rangle$ (fractionally an overestimate of about 0.75 %).

We should expect offsets between observations and predictions in other stars. If the Sun is typical, the offsets for the frequencies will be many times the sizes of the expected frequency uncertainties. The achievable precision in the large separations is nowhere near as good, and so there fractional offsets would in many cases be comparable to the observed uncertainties. Failure to account for these offsets will lead to errors in the estimated stellar properties. But how important might those errors be?

Consider first a simple case, estimation of the mean stellar density $\langle \rho \rangle$, taking the Sun as an example. We assume that for small fractional changes – e.g., those describing the differences between a reasonably good model and observations – homologous scaling of the frequencies holds to good approximation. This implies that $\delta\nu_{nl}/\nu_{nl} \simeq \delta \langle \Delta\nu_{nl} \rangle / \langle \Delta\nu_{nl} \rangle \simeq 1/2 \delta \langle \rho \rangle / \langle \rho \rangle$. The fractional solar surface term offsets in ν_{nl} (for frequencies close to ν_{\max}) and $\langle \Delta\nu_{nl} \rangle$ quoted above imply inferred densities would be in error by, respectively, a few tenths of a percent when using frequencies, and 1 to 2 % when using the average large separation. From Equations 13 and 14, one might naively expect fractional errors of roughly similar size and double the size in radius and mass, respectively.

Provided the fractional offset in the stellar $\langle \Delta\nu_{nl} \rangle$ is similar to the fractional

offset for the Sun, one can actually suppress the effects of the surface term quite straightforwardly when the large separation is used (and remove it when analysing the Sun). When using the scaling relations, one should scale the observed separation against the observed $\langle \Delta\nu_{nl} \rangle_{\odot}$. When using stellar-model calculated frequencies to estimate $\langle \Delta\nu_{nl} \rangle$ in the grid-based method, one should again scale the observed separation against $\langle \Delta\nu_{nl} \rangle_{\odot}$ whilst making sure that each model-calculated average separation is scaled against a solar-model average separation made from a properly calibrated solar model having the same input physics as the model grid. Any residual bias in the estimated properties will be due to fractional differences between the solar and stellar surface term, all other things being equal. Even with a surface term twice as large as solar, errors of only a few percent would result.

Given that the typical precision in direct-method and grid-based estimated properties is at the several percent level, the surface term effects are most likely not a significant cause for concern, with bias from other ingredients of the modelling being more of an issue. What of the individual frequencies? Kjeldsen, Bedding & Christensen-Dalsgaard (2008) have proposed an empirically motivated procedure to correct individual frequencies. Since the solar surface term may be described fairly well by a power law in frequency, they suggest in effect treating the surface term of other stars as a homologously scaled version of the solar offset. Application of the Kjeldsen et al. correction to ground-based data on stars with similar T_{eff} and $\log g$ (i.e., similar ν_{ac} and hence ν_{max}) to the Sun has indicated similar surface-term properties in those stars, while on a larger sample of 22 solar-type stars observed by *Kepler* the average size of the best-fitting surface term was found to increase in magnitude with increasing $\log g$ (Mathur et al. 2012). Moreover, further inspection of

these data shows that the ratio of the absolute size of the term to ν_{\max} is almost constant. It does however remain to be seen whether this result instead carries information related largely to other shortcomings of the stellar models, not necessarily information associated with the surface term (i.e., due to degeneracies from the modelling). It must be borne in mind that different choices made in the construction of stellar models can impact not only on the shape but possibly also on the sign of the surface term. One needs only compare the surface term of different standard solar models to see that for some the surface term can be positive rather than negative up to frequencies close to $\nu_{\max\odot}$ (albeit at a level smaller than at higher frequencies).

Results from 3D numerical simulations of convection will provide important input, e.g., as discussed by Goupil et al. (2011). But what is also needed are good asteroseismic targets with independently measured accurate (and precise) properties, which would allow an exploration of the model degeneracies associated with the surface term.

Meanwhile, an obvious way to circumvent the problems presented by the surface term is to instead employ frequency separation ratios in the modelling, as first pointed out by Roxburgh & Vorontsov (2003). Recall that these ratios are somewhat independent of the structure of the near-surface layers.

5.2 Use of signatures of modes of mixed character

As a star evolves and its central regions contract the gravitational acceleration near the core increases and so do the frequencies of gravity modes (see Equations 10 to 12). Eventually, typically in the subgiant phase, g-mode frequencies increase sufficiently to give interactions with acoustic modes of the same angular

degree. The resulting frequency spectrum is thus not merely a simple superposition of p and g modes but is determined by the coupling strength of the interacting modes. When the observed mixed modes are mostly dominated by p-mode as opposed to g-mode characteristics information on the interactions is most easily recovered by studying departures from a constant frequency spacing. Visually, one could inspect an échelle diagram (see Section 2) folded by the average large frequency separation (e.g., see Metcalfe et al. 2010b as applied to the *Kepler* subgiant KIC 11026764). When g-mode characteristics dominate, it is better to fold in period, using the average period spacing (Bedding 2011).

Mode bumping can affect the frequencies of several p (g) modes in consecutive orders dependent on the coupling strength and the density of modes in the spectrum. In favourable cases where several perturbed p (or g) modes may be detected information on the coupling strength, and on the underlying unperturbed p-mode and g-mode frequencies, may be inferred by modelling the interaction between the g-mode and p-mode cavities (Unno et al. 1989, Bedding 2011, Deheuvels & Michel 2011, Christensen-Dalsgaard & Thompson 2011, Mosser et al. 2012a,c). This approach, when applicable, provides an invaluable tool to explore and exploit the diagnostic potential of using modes of mixed character as probes of internal properties, such as the behaviour of N in the deep stellar interior, and the characteristics of the evanescent region between the p- and g-mode propagation cavities. The full potential of *Kepler* and CoRoT data is still to be exploited. However, even from analyses of the first few months of observations there were cases where the estimated frequencies were already of sufficient quality to enable detailed studies of the coupling strength of interacting modes, including the frequencies of the unperturbed g modes in subgiants (Deheuvels & Michel 2011,

Benomar et al. 2012).

Provided that the underlying coupling model is accurate, information on the frequency of the underlying g modes, and on the coupling itself, in principle allows robust inference to be made on the fundamental stellar properties (Deheuvels & Michel 2011). In subgiants and low-luminosity giants of a given mass and chemical composition the frequency of a g mode (or the period spacing of g modes, when detectable) is a monotonic function of age. By fitting simultaneously the frequency of the avoided crossing and the average large frequency separation a precise value of the age and mass can be determined for a given chemical composition and input physics, as has been shown for the subgiant HD 49385 observed by CoRoT (Deheuvels & Michel 2011, Deheuvels et al. 2012). The coupling strength is also a promising proxy of stellar mass during the subgiant phase, as demonstrated by Benomar et al. (2012) for a selection of subgiants observed by *Kepler*, CoRoT and ground-based telescopes.

Following the subgiant phase, the period spacing of the g modes decreases throughout evolution on the RGB as the stars develop very compact helium cores. At the same time large frequency separations decrease in response to significant expansion of the stellar radii, hence the number of g modes per large separation increases markedly leading to very dense spectra of modes.

In perhaps the most significant asteroseismic result of recent years, *Kepler* data were used to show that observed g-mode period spacings are substantially higher for helium-core-burning stars in the red clump (RC) than for stars ascending the RGB, providing a clear way to discriminate stars that otherwise show very similar surface properties (Bedding et al. 2011). Theoretical work (Montalbán et al. 2010) had already indicated that the properties of the $l = 1$ modes were expected

to be sensitive to the evolutionary state of giants. Detection of the dense spectra of $l = 1$ modes and measurement of the period spacings (Bedding et al. 2011, Beck et al. 2011) revealed a clear division of the observed spacings and comparison with predictions from stellar evolutionary models allowed the results to be properly interpreted. Similar results on the period spacings using CoRoT data were subsequently obtained by Mosser et al. (2011a).

The typical period spacing in low-mass RGB stars (at the luminosity of stars in the RC) is $\simeq 50$ to 70 s, while in the RC the average spacing increases to a few-hundred seconds. The differences may be understood as follows: The helium core experiences a sudden expansion following ignition of helium-burning reactions. Re-adjustment of the stellar structure due to the increased luminosity in the core results in a significant decrease of N in the central regions, giving rise to an increased period spacing. In addition to the decreased core density, the release of energy from the helium-burning nuclear reactions leads to the onset of convection in the energy-generating core, contributing to an even larger increase of the spacing. (See Christensen-Dalsgaard 2011 and Montalbán et al. 2013 for further discussion.)

A firm identification of the evolutionary state of thousands of giants has wide-ranging implications, from the study of stellar populations (which we discuss in Section 7), to providing a much larger sample on which to test the efficiency of extra mixing mechanisms in the giant phase (e.g., Charbonnel 2005). Moreover, a carefully chosen sample of RGB and RC stars could be used to quantify the effects of mass loss on the RGB (Mosser et al. 2011a).

Full exploration of the diagnostic potential of the period spacings – including detailed comparison of observations and model predictions – promises to

shed light on the detailed core properties, including helping to constrain the efficiency of mixing processes in low- and intermediate-mass stars. As noticed in Montalbán et al. (2013) the average value of the period spacing in helium-burning intermediate-mass stars is tightly correlated with the mass of the helium core. An accurate calibration of the relation between core-helium mass and stellar mass for different metallicities will provide stringent constraints on the efficiency of extra mixing that occurred in the near-core regions during the main sequence phase (e.g., see Girardi 1999). Moreover, in core-helium burning stars the period spacing is sensitive to the size of the adiabatically stratified convective core, and to the temperature stratification in the near-core regions. A detailed characterisation of such regions promises to reduce current uncertainties on the required extra mixing, and its efficiency during the core-helium burning phase (see Salaris 2012 for a recent review). Such uncertainties have implications for the total helium-burning lifetimes, the resulting carbon-oxygen profile and subsequent evolutionary phases.

Finally, we note the exciting possibility of detecting stars in the fast evolutionary phases between the occurrence of the first helium flash and the quiet RC phase (Bildsten et al. 2012), where data on the period spacings could add significant knowledge to our understanding of the structural changes that follow helium ignition in low-mass stars (Weiss 2012).

5.3 Use of signatures of abrupt structural variation

Regions of stellar interiors where the structure changes abruptly, such as the boundaries of convective regions, give rise to departures from the regular frequency separations implied by an asymptotic description. Careful measurement of these signatures – sometimes referred to as glitches – not only has the poten-

tial to provide additional information on the stellar properties, but also elucidates other important parameters and physical properties of the stars. There are signatures left by the ionization of helium in the near-surface layers of the stars. Measurements of these signatures should allow tight constraints to be placed on the helium abundance, something that would not otherwise be possible in such cool stars (because the ionization temperatures are too high to yield usable photospheric lines for spectroscopy). And as noted above, there are also signatures left by the locations of convective boundaries. It is therefore possible to pinpoint the lower boundaries of convective envelopes, potentially important information for dynamo studies of cool stars. Furthermore, it is also possible to estimate the sizes of convective cores. Measurement of the sizes of these cores, and the overshoot of the convective motions into the layers above, is important because it can provide a more accurate calibration of the ages of the affected stars. The mixing implied by the convective cores, and the possibility of mixing of fresh hydrogen fuel into the nuclear burning cores – courtesy of the regions of overshoot – affects the main-sequence lifetimes.

5.3.1 SIGNATURES FROM STELLAR ENVELOPES The characteristics of the signatures imposed on the mode frequencies depend on the properties and locations of the regions of abrupt structural change. When the regions lie well within the mode cavities a periodic component is manifest in the frequencies ν_{nl} , which is proportional to

$$\sin(4\pi\nu_{nl}\tau + \phi), \quad (17)$$

where

$$\tau = \int_r^R \frac{dr}{c} \quad (18)$$

is the acoustic depth of the glitch feature, r is the corresponding location in radius, c is the sound speed, and ϕ is a phase offset (Vorontsov 1988, Gough 1990). The “period” of the signature induced in the frequencies, which equals 2τ , provides information on the location of the region. The amplitude of the signature provides a measure of the size of the structural perturbation, while the decrease in amplitude with increasing frequency gives information on the radial extent of the glitch. Two signatures of this type have already been well studied in the solar case: one due to the sharp variation in the gradient of the sound speed at the base of the convective envelope; and another due to changes in the adiabatic exponent in the near-surface helium ionization zones (see Christensen-Dalsgaard 2002, and references therein).

While the periodic signatures from the helium ionization zones may already be readily apparent in the large frequency separations $\Delta\nu_{nl}$, their signals may be better isolated by, for example, taking second differences of frequencies of modes having the same angular degree l , i.e., $\Delta_2\nu_{nl} = \nu_{n-1l} - 2\nu_{nl} + \nu_{n+1l}$, or by subtracting the frequencies from a smoothly varying function in the overtone number, n . The signature from the base of the convective envelope is also apparent in the second differences, although at a reduced amplitude compared to the helium signatures. Potentially better diagnostics from which to extract the convective-envelope signature are the frequency separation ratios constructed by using the $l = 0$ and $l = 1$ modes (Roxburgh 2009), i.e., $r_{01}(n) = \delta\nu_{01}(n)/\Delta\nu_1(n)$ and $r_{10}(n) = \delta\nu_{10}(n)/\Delta\nu_0(n + 1)$. Since the small and large separations are affected in a similar way by the near-surface layers, signatures from the near-surface ionization zones are largely suppressed in the ratios, leaving the signature from the base of the convective envelope. Use of the separation ratios gives a

periodic signal in the frequencies equal to twice the acoustic radius, $2t$, not twice the acoustic depth, 2τ . Acoustic radii, t , are defined by:

$$t = T_0 - \tau, \quad (19)$$

where the acoustic radius of the star, T_0 , is given by

$$T_0 = \int_0^R \frac{dr}{c} = 1/(2\Delta\nu) \simeq 1/(2\langle\Delta\nu_{nl}\rangle). \quad (20)$$

Figure 6 shows the convection-zone-base glitch signature of the main-sequence *Kepler* target HD 173701 (KIC 8006161; see Appourchaux et al. 2012, Mazumdar et al. 2012b), as observed in the frequency separation ratios made from the star’s estimated oscillation frequencies.

Since both τ and T_0 contain contributions from the hard-to-model near-surface layers, translation to the radii t when using frequencies or second differences as observables will suppress the surface contribution, in principle making comparisons with model predictions more straightforward. An important caveat worth adding is that use of the different frequency diagnostics (or combinations) outlined above will give small differences in the results, since the exact properties of the glitches depend on the chosen diagnostic. For example, explicit in the construction of the diagnostic used by Houdek & Gough (2007) is an assumed matching of the stellar interior to a model atmosphere, where the upper reflecting layer for many modes lies. Other methods may not take explicit account of the exact location of the reflecting surface. That said, these differences are typically rather small, and do not compromise the precision of inferences made at the few percent level.

The acoustic depth of the base of the solar convective envelope lies at $\tau_{\text{BCZ}} \approx 2300$ s, and produces a glitch signal with an amplitude of approximately $0.1 \mu\text{Hz}$ in

the frequencies. The solar He II ionization zone produces a signal at $\tau_{\text{HeII}} \approx 700$ s, and a glitch-signal amplitude of approximately $1 \mu\text{Hz}$.

The key to extracting the envelope glitch signatures is to have sufficient precision in estimates of the frequencies, and data on a sufficient number of overtones in the spectrum. Ideally, one typically requires individual frequency uncertainties of the order of a few tenths of a μHz or lower, which demands multi-month observations of the stars. The resolution achievable in period will correspond to $\simeq 1/(\Delta n \times \langle \Delta \nu_{nl} \rangle)$, i.e., the total range in frequency spanned by the useable frequencies, where Δn is the number of overtones covered. When the S/N in the glitch signatures is good, the resolution largely fixes the uncertainty in the estimated acoustic depth.

The range of depths accessible to the analysis is determined by the large frequency separation of the star. One may cast a discussion on the limits in terms of the Nyquist-Shannon sampling theorem. When individual frequencies are available on $l = 0$ and $l = 1$ modes the diagnostics data are sampled in frequency at an approximately regular interval of $\simeq \langle \Delta \nu_{nl} \rangle / 2$, implying a Nyquist “period” of $1 / \langle \Delta \nu_{nl} \rangle$. This sets a notional upper limit on measureable “periods” of $\simeq 2T_0 \simeq 1 / \langle \Delta \nu_{nl} \rangle$, and hence an upper limit on measureable acoustic depths of $\simeq T_0 \simeq 1 / (2 \langle \Delta \nu_{nl} \rangle)$. In subgiants and red giants that show mixed modes one may not have the luxury of being able to use non-radial modes to construct glitch diagnostics since they will show the effects of mode coupling. The sampling in frequency is then only $\simeq \langle \Delta \nu_{nl} \rangle$, which halves the upper-limit measureable acoustic depth and it is then not possible to distinguish between a structural glitch located at an acoustic depth τ , and one located at an acoustic depth $T_0 - \tau$. We return later in the section to consider the case of evolved stars.

In solar-type stars the base of the convective envelope is located at an acoustic depth of roughly $\approx T_0/2$ or deeper, and so $l = 1$ modes are needed to avoid potential aliasing problems. Of all the solar-type stars, early F-type stars have the shallowest convective envelopes. Since the ratio of the envelope and He II zone depths is much smaller than in Sun-like analogues, it can be hard to disentangle the signatures (most notably in stars with $M \geq 1.4 M_\odot$). Even though the separation of the signals is in contrast most pronounced in later-type, lower-mass dwarfs, the amplitude of the convective envelope signature is then very weak and hence more challenging to extract.

The first measurements of the envelope glitch signatures of a solar-type star other than the Sun were made by Mazumdar et al. (2012a). They extracted the envelope and He II signatures of the F-type star HD49933 using estimated frequencies obtained from 180 days of data collected by CoRoT. The analysis proved challenging for two reasons: first, due to the close correspondance of the glitch periods (see above); and second, due to the large frequency uncertainties from the heavy damping of the modes (a notable characteristic of F-type stars). This resulted in large uncertainties on the estimated envelope depth.

Thanks to *Kepler*, more precise frequencies (from longer datasets) are now available on a large ensemble of solar-type stars. Mazumdar et al. (2012b) analyzed a representative sample of 19 of these stars, and demonstrated that it is already possible to extract very precise estimates of the glitch signature properties. Four different techniques of analysis were applied to extract the glitch signatures, using different combinations of the observed frequencies, as based on the methods outlined in Houdek & Gough (2007), Monteiro, Christensen-Dalsgaard & Thompson (2000), Mazumdar et al. (2012a) and Roxburgh (2009). Very good agreement was

found in the inferred glitch properties, giving confidence in the extracted values. For example, acoustic convective envelope depths were estimated to a typical precision of a few percent.

The results from Mazumdar et al. (2012b) have validated the robustness of the analysis techniques, and indicate that we are now in a position to apply them to, and exploit the results from, more than 100 solar-type stars with multi-month *Kepler* data. The *Kepler* ensemble will provide a comprehensive set of convective envelope depths for testing stellar evolution theory, and for validating stellar dynamo models. Results of those tests should also open the possibility to use the estimated envelope and He II depths as input to help constrain both the gross stellar properties, and interiors structure (Mazumdar 2005). It will also be possible to use the extracted envelope glitch signatures to place constraints on overshoot into the radiative interiors (e.g., Monteiro, Christensen-Dalsgaard & Thompson 2000). Moreover, as pointed out by Houdek & Gough (2007) and Houdek & Gough (2011), careful measurement and subsequent removal of glitch signatures from the mode frequencies will in principle provide cleaner inference on the stellar properties, notably age, when those frequencies are used to model stars.

Extraction of the He II signatures allows an estimate to be made of the helium abundances in the stellar envelopes, as discussed by, for example, Basu et al. (2004) and Monteiro & Thompson (2005). If we assume that the stellar mass and radius have already been determined to a fractional precision of $\approx 10\%$ and 5% , respectively – for example from the standard asteroseismic methods outlined in previous sections – it should be possible to use the measured amplitude of the glitch signal to constrain the envelope helium abundance to better than 10% .

Evolved stars present different challenges for the analysis of glitch signatures.

First, as noted above, significant coupling may render mixed modes poor diagnostics of the sought-for signatures. Exceptions will be when the coupling with g modes is weak, e.g., in $l = 1$ modes in luminous RGB stars, or in $l = 2$ modes. Second, the number of acoustic modes trapped in the stellar interior decreases as the stellar radius increases (e.g., see Christensen-Dalsgaard 2011). This is because the frequency domain covered by the acoustic modes scales approximately as ν_{\max} , and since the modes are spaced according to $\Delta\nu$ the number of overtones observed will scale as $(\nu_{\max}/\Delta\nu) \propto M^{1/2}R^{-1/2}T_{\text{eff}}^{-1/2}$. As stars evolve up the RGB, we might therefore expect to observe fewer overtones than in main-sequence stars, which makes extraction of periodic signatures in frequency more challenging. It is worth adding that the S/N in those modes that are detected will be higher (and peak linewidths narrower) than in main-sequence stars on account of the higher mode amplitudes (and lower damping rates) shown by evolved stars. Third, as a star evolves off the main sequence and the convective envelope deepens, the base of the envelope is displaced to greater acoustic depths (typically to $\geq 0.9T_0$, depending on the mass, chemical composition and evolutionary state). In this respect the detection of seismic signatures of helium ionisation is simpler for giants than for solar-type stars, since the He signatures do not have to be disentangled from the convective envelope signatures.

Glitch signatures have already been detected in red giant data collected by CoRoT, the first published example being HR 7349 (Miglio et al. 2010). Given the quality of the *Kepler* data, we may expect signatures to be detected and characterised precisely in a large number of giants, opening the possibility to constrain the envelope helium abundance in old stars (although further work is needed to understand how parameters extracted on the signatures impact on the

accuracy and precision of estimated helium abundances).

5.3.2 SIGNATURES FROM STELLAR CORES When regions of abrupt structural change do not lie well within the mode cavities the signatures they leave in the mode frequencies are more subtle. This is the case for the signatures left by convective cores found in solar-type stars slightly more massive than the Sun.

Seismic diagnostics of convective cores are particularly important (Noels et al. 2010). Several physical processes – e.g., rotation, overshooting, semiconvection and diffusion – may alter the shape of the chemical composition profile near the border of a convective core, mainly through full or partial mixing of the radiatively stable layers beyond the formal boundary of the convective region, as set by the Schwarzschild criterion. Constraining the efficiency of such extra mixing has wide relevance, most obviously since it would decrease systematic uncertainties on the age determinations of the affected main-sequence stars. There are significant uncertainties in the modelling of transport processes in stellar interiors (e.g., due to the lack of a satisfactory theory for convection); seismic constraints on near-core mixing may be used to test such models, and to improve, eventually, our understanding of stellar physics.

Comparisons of theoretical models and “classical” non-seismic observations of stars show clearly that standard stellar models underestimate the size of the centrally mixed region, for example from stringent observational constraints provided by detached eclipsing binaries and open clusters (e.g., see Andersen, Clausen & Nordstrom 1990; Ribas, Jordi & Giménez 2000). While the need for extra mixing is generally accepted, the calibration of its efficiency for stars of different mass and chemical composition is very uncertain, in particular in the mass range 1.1 to 1.6 M_{\odot} (e.g., see Demarque et al. 2004; VandenBerg & Stetson 2004; VandenBerg, Bergbusch & Dowler

2006). Moreover, there is no clear consensus regarding the physical processes responsible for the required extra-mixing that is missing in the standard models. Possibilities include overshooting in its classical and diffusive flavors (e.g. Maeder 1975, Ventura et al. 1998), microscopic diffusion (Michaud et al. 2004), rotationally induced mixing (e.g., see Maeder & Meynet 2000, Mathis, Palacios & Zahn 2004, and references therein), and mixing generated by propagation of internal waves (e.g. Young et al. 2003, Talon & Charbonnel 2005).

A necessary condition for seismology to act as a diagnostic is that the mixing process leaves a distinct signature in the chemical composition profile, hence in the sound speed or N , which acoustic and gravity modes are sensitive to. Several studies have proposed and discussed the theoretical potential of diagnostics for solar-type stars based upon use of the small frequency separations, frequency separation ratios (see Section 2), and other more elaborate combinations of individual frequencies (Popielski & Dziembowski 2005, Mazumdar et al. 2006, Cunha & Metcalfe 2007, Cunha & Brandão 2011, Silva Aguirre et al. 2011a). The most recent work has focussed in particular on developing diagnostics based on use of $l = 0$ and $l = 1$ modes. These modes have significantly higher visibilities in the *Kepler* and CoRoT data than do modes of higher l . Diagnostics are now beginning to be applied to the space-based data, which have the requisite frequency precision not achieved from ground-based observations. A possible exception involving ground-based data is the well-studied binary α Cen where tight complementary constraints (including masses from the analysis of the visual binary orbit) are available. de Meulenaer et al. (2010) showed that the small frequency separations $\delta\nu_{01}(n)$ extracted from ground-based data on α Cen A were at odds with models computed using a substantial amount of extra mixing in the core.

In solar-type stars, an asymptotic formalism of the frequencies based on a description of the internal phase shifts in principle provides the foundations for carrying out inverse analyses to infer the structures of stellar cores, using only low- l modes (Roxburgh 2010). The observation of mixed modes would help to dramatically improve the quality of the inversions, since they provide kernels localised in the core of the star (Basu, Christensen-Dalsgaard & Thompson 2002).

Constraints on the detailed properties of mixing in the near-core regions may also be inferred from the analysis of data on more evolved stars showing mixed modes. Mixed modes observed in subgiant stars result from coupling of high-order p modes and low-order g modes. The frequencies of the latter may present significant deviations from the asymptotic limit and therefore bear information on abrupt structural variations related to the chemical composition gradient in the near-core regions (which controls N). Such a gradient is determined primarily by the evolutionary state, but can also be modified by different mixing processes taking place in the radiative interior. If the profile of N changes because of a different composition gradient, then we can expect a signature of the different mixing processes to be present in the frequencies of the mixed modes.

Seismic signatures of a smooth composition profile arising from non-instantaneous mixing were investigated by Miglio, Montalbán & Maceroni (2007), while Deheuvels & Michel (2011) have also highlighted the potential effects of diffusion on the detailed behaviour of N near the core. These studies suggest that such subtle effects may be detectable in stars that are evolved enough to present avoided crossings, yet sufficiently close to the end of the main sequence that the mean molecular weight profile has not yet been significantly modified by nuclear reactions in a surrounding shell.

As discussed in Section 5.2, comparison of observed and model-predicted frequencies of giants should provide information on mixing processes occurring during the core-helium burning phase, which can have a significant impact on later evolutionary phases (e.g., see Straniero et al. 2003).

Finally in this section we note that rotation may also act to induce deep-seated mixing in stars with radiative cores. Eggenberger et al. (2010) studied the effects of this by comparing rotating and non-rotating models having the same fundamental properties. They noticed that rotational mixing increased the average small separations and frequency separation ratios, and lead to a slightly steeper slope of the small separations with frequency, reflecting the impact of rotation on the chemical composition gradients and in particular changes in the abundance of hydrogen in the central parts of the star.

5.4 Inferences on internal rotation

Despite the importance of effects of rotation in the formation and evolution of stars (e.g., see Pinsonneault 1997, Maeder & Meynet 2000) little is known about the efficiency of, and interplay between, the physical processes regulating the transport of angular momentum in stellar interiors. Observational constraints on the impact of rotation during stellar evolution are generally limited to surface abundances signatures of deep mixing, and to measurements of the surface rotation of stars in different evolutionary states.

A notable exception is of course the Sun, where helioseismic analysis of the frequency splittings of non-radial p modes has provided a detailed picture of rotation in the solar interior (e.g., see Thompson et al. 2003, Howe 2009). Helioseismology revealed the solar tachocline, a narrow region in the stably stratified layer just

beneath the base of the convective envelope which mediates the transition from differential rotation in the envelope to a solid-body-like profile in the radiative interior and is believed to play an integral rôle in dynamo action (Ossendrijver 2003). Helioseismic inversions showed that the solid-body-like profile persists down to at least $R \sim 0.2 R_{\odot}$ (deeper down inferences are rather uncertain), results that present severe challenges to models of angular momentum transfer in the solar interior (e.g., see Pinsonneault et al. 1989).

Long, continuous datasets are needed to extract accurate and precise estimates of the rotational frequency splittings of low- l p modes in main-sequence stars. The frequency splittings, $\delta\nu_{nlm}$, will typically vary from a few μHz (in more massive, and/or very young solar-type stars) down to a fraction of a μHz (in less massive, and/or more mature solar-type stars; see inset to Figure 1). The splittings may often be of comparable size to the linewidths of the damped modes in the frequency-power spectrum, which will in some cases prevent robust extraction of the splittings and in others means that care is needed to deal with potential biases. Extensive testing with Sun-as-a-star and artificial data mean that these problems are well understood (Chaplin et al. 2006).

The robust detection of variations of p-mode splittings with frequency, angular degree and azimuthal order will be challenging, but promises to provide information on near-surface magnetic fields (which can contribute to the splittings) as well as internal differential rotation (much harder). A first obvious exercise using the *Kepler* ensemble will be to compare the average frequency splittings with measures of surface rotation periods.

While the frequency splittings of p modes observed in main-sequence stars are largely determined by the rotation profile in the stellar envelope (as in the

case of the Sun), the situation is different in the case of evolved stars where modes of mixed character are sensitive to the rotation in deeper-lying layers. As noted in Section 3, the fact that these modes are also less heavily damped than pure p modes means they present very narrow peaks in the frequency-power spectrum. This makes extraction of the observed frequency splittings in principle more straightforward than in main-sequence stars. Long datasets are nevertheless still required, and during some evolutionary epochs (e.g., giants in the RC) the complicated appearance of the oscillation spectra can present additional challenges for disentangling the splittings.

Recently, Beck et al. (2012) measured rotational splittings of mixed modes in three low-luminosity red-giant stars observed with *Kepler*. Mixed modes were identified in each power spectrum as dense clusters of $l = 1$ modes. The mode at the centre of each cluster is dominated by p-mode characteristics, and is hence most sensitive to the external layers. Adjacent modes are more g-mode-like in character, and so their rotational kernels (Equation 6) are localised predominantly in the central regions of the star. Through a first comparison with rotational kernels representative of the modes observed in one of the giants (KIC 8366239), the authors found evidence for a core rotating at least ten-times faster than the surface.

Eggenberger, Montalbán & Miglio (2012) compared the observed splittings with those predicted by models including meridional circulation and shear instability. They concluded that these processes alone produce an insufficient coupling to account for the rotational splittings observed in KIC 8366239, and that an additional mechanism for the transport of angular momentum must operate in stellar interiors during post-main sequence evolution. Moreover, by comparing the ratio

of splittings for p- and g-dominated modes, they estimated the efficiency of this additional physical process.

Deheuvels et al. (2012) also recently reported the detection of rotationally split modes in HIP 92775 (KIC 7341231), a halo star at the base of the RGB. By applying various inversion techniques and assumptions on the functional form of the rotation profile, they could set quantitative constraints on the internal rotation profile of the star. This led to a robust inference on the rotation of the core, and an upper limit to the surface rotation, establishing that in HIP 92775 the core rotates at least five-times faster than the surface. As pointed out by the authors, while the rotation period of the core could be robustly derived, weaker constraints were obtained on the surface rotation, due to the fact that rotational splittings of dipolar modes detected in these low-luminosity giants are significantly contaminated by the core rotation. In the future the detection of rotationally split $l = 2$ modes, and splittings in stars with different trapping properties, should provide information on rotation profiles in the stellar envelopes (including potentially differential rotation).

Mosser et al. (2012b) estimated average rotational frequency splittings for around 300 giants, providing direct constraints on the evolution of the mean core rotation for stars in the red-giant phase. Comparison of the measured core rotation rates for RGB and RC stars provides evidence for core spin-down in the final phases of evolution on the RGB.

Detailed comparisons with theoretical predictions of internal rotational profiles at different evolutionary states are needed to quantify the effects of additional processes transporting angular momentum in radiative (Charbonnel & Talon 2005, Gough & McIntyre 1998, Mathis 2009) and convective regions (Palacios 2012).

Moreover, in order to achieve a fully consistent physical picture of transport of chemicals and angular momentum in stars of different masses, chemical compositions, and evolutionary stages, models will have to reproduce not only seismic constraints on the internal rotational profile but also chemical signatures of deep mixing obtained via spectroscopic methods (e.g., see Smiljanic et al. 2009, and references therein).

6 Asteroseismology, exoplanets, and stellar activity studies

Asteroseismology can be particularly powerful when it is applied to stars that are exoplanet hosts. It can provide the accurate and precise estimates of the stellar properties (i.e., density, surface gravity, mass, radius and age) that are needed to make robust inference on the properties of the planets, and information on the internal rotation and stellar angle of inclination to help better understand the evolutionary dynamics of the systems. Moreover, asteroseismology can be used to probe levels of near-surface magnetic activity, interior-atmosphere linkages, and stellar activity cycles, all relevant to understanding the influence that stars have on their local environments, where planets are found.

The first asteroseismic studies of exoplanet hosts showing solar-like oscillations used ground-based Doppler velocity observations of μ Arae (Bouchy et al. 2005, Bazot et al. 2005, Soriano & Vauclair 2010) and ι Hor (Vauclair et al. 2008). The Hubble Space Telescope fine guidance sensor provided several days of asteroseismic data on the solar-type host HD 17156 (Gilliland et al. 2011). Studies of four other known exoplanet hosts were made possible by early prioritisation of targets observed by CoRoT (HD52265; see Ballot et al. 2011, Escobar et al. 2012) and by *Kepler* (HAT-P-7, HAT-P-11 and TrES-2; see Christensen-Dalsgaard et al.

2010).

Kepler has further opened the possibilities to combine exoplanet studies and asteroseismology, with (at the time of writing) solar-like oscillations detected in around 80 stars which also have single or multiple candidate, validated or confirmed transiting exoplanets (Huber et al. 2013). These asteroseismic *Kepler* Objects of Interest (KOIs) span the *Kepler* apparent magnitude range $7.4 \leq K_p \leq 13.5$, the peak of the sample lying around $K_p \simeq 12$. This 80-strong sample of asteroseismic KOIs provides a unique ensemble with extremely well-constrained stellar properties.

Kepler's transit observations provide a direct estimate of R_p/R , i.e., the ratio of the radii of the planet and star, hence accurate and precise radii from asteroseismology allow tight constraints to be placed on the absolute sizes of the planets. The stellar radius is also required to fix the stellar luminosity and hence the location of the habitable zone around the star. There are already several examples in the literature where asteroseismically estimated stellar radii put tight constraints on the radii of small planets, e.g., Kepler-10b, *Kepler*'s first rocky exoplanet (Batalha et al. 2011), and Kepler-21b (Howell et al. 2012). Particularly noteworthy was Kepler-22b (Borucki et al. 2012), *Kepler*'s first validated planet lying in the habitable zone of its host star. This Sun-like analogue is quite faint for asteroseismology, and provided an excellent example of how a detection of just the large frequency separation was sufficient to get a good estimate of the stellar radius (the modes were too weak to estimate individual frequencies).

In systems that are bright enough for follow-up radial velocity observations those velocity data may be combined with the transit data to estimate planetary masses, M_p . An accurate estimate of the stellar mass, M , is required (which

asteroseismology can again provide) with the inferred planetary mass scaling with the stellar mass according to $M_p \propto M^{2/3}$. A recent example is the Kepler-68 system (Gilliland et al. 2013).

When usable radial velocity data cannot be obtained (due to a combination of the faintness of the star, and small sizes of the planets) *Kepler* has shown how detected transit timing variations (TTVs) in multi-planet systems may be used to help constrain the planetary properties. These TTVs correspond to deviations from strictly periodic transit intervals, and arise due to the mutual gravitational interactions of the planets. So-called photodynamical models combine information from the observed transits – including data on the TTVs – with the estimated properties of the host star. Here, the inferred planetary masses depend on the stellar mass, via $M_p \propto M$. Carter et al. (2012) presented the first example of combining TTVs and asteroseismology, the Kepler-36 system containing two planets. The small uncertainties on the stellar mass and radius proved crucial to constraining the planet masses and radii to better than 8% and 3% respectively, helping to confirm the unusual nature of the system (planets having markedly different densities lying in closely spaced orbits).

Stellar ages estimated from asteroseismology of course provide upper-limit age estimates for the planets. This information is of particular interest for cases where planets are potentially habitable, and for those developing planet evolutionary models, but is also relevant to calculations of the long-term stability of discovered systems, e.g., for confirming that inferred configurations are stable on the required timescales (as in the case of Kepler-36) or for ruling out potential configurations that may be unstable in systems where there are degeneracies in the inferred best-fitting solutions.

Asteroseismology may also be used to improve the accuracy of spectroscopic estimates of temperature and metallicity, which are needed for analysis of the host stars. Spectroscopic $\log g$ can be very uncertain and inaccuracies can lead to bias in estimates of T_{eff} and $[\text{Fe}/\text{H}]$ due to strong correlations in the analysis. In the case of the asteroseismic KOIs (e.g., Borucki et al. 2012, Carter et al. 2012, Huber et al. 2013), estimates of $\log g$ from asteroseismology (which used initial estimates of T_{eff} and $[\text{Fe}/\text{H}]$ from spectroscopy as inputs) were used as a strong prior on $\log g$ in re-analysis of the spectroscopic data. Only one iteration was needed to reach convergence in the asteroseismically estimated stellar properties. A similar approach has been adopted using stellar densities measured from transit lightcurves (Torres et al. 2012).

One of the most exciting areas where asteroseismology may be brought to bear is to provide information on the spin-orbit alignments of exoplanet systems. Asteroseismology may be applied to estimate the angle i between the stellar rotation axis and the line-of-sight. When applied to transiting systems, where the orbital plane of the planets must be close to edge-on, an estimated i significantly different from 90 degrees – such that the rotation axis is well inclined relative to the plane of the sky – will imply a spin-orbit misalignment.

Asteroseismic estimation of i rests on our ability to resolve and extract signatures of rotation in the non-radial modes of the oscillation spectrum. The mode patterns of the non-radial modes are non spherically symmetric, and hence the observed amplitudes of the modes depend on the viewing angle. For the slow to moderate rates of rotation expected in solar-like oscillators, measurement of the observed relative power of the different azimuthal components in each non-radial mode provides a direct estimate of i (for a detailed discussion of the

method, see Gizon & Solanki 2003, Ballot, García & Lambert 2006, Ballot et al. 2008, Chaplin et al. 2013). In the best cases, asteroseismology can constrain i to an uncertainty of just a few degrees. The analysis requires bright targets and long-duration timeseries to give the requisite signal-to-noise and frequency resolution for extracting clear signatures of rotation in the oscillation spectrum.

When peak-bagging models are fitted to the modes to extract the required information, the maximized likelihoods exhibit strong correlations between the rotational frequency splittings $\delta\nu_s$ and $\sin i$. This means that when the S/N in the modes or the length of the dataset is insufficient to extract a unique solution for the splitting and angle it is still often possible to estimate the product $\delta\nu_s \sin i$. *Kepler* data may also provide estimates of the surface rotation period, P_{rot} , from rotational modulation of starspots and active regions. Hence, even when a unique asteroseismic solution for i is unavailable, the observed seismic product $\delta\nu_s \sin i$ can be combined with the observed P_{rot} to estimate the sine of the angle, i.e., from $\sin i = (\delta\nu_s \sin i)P_{\text{rot}}$. This is similar to the method that combines P_{rot} with $v \sin i$ from spectroscopy (e.g., see Hirano et al. 2012 for examples using *Kepler* data). Implicit is the assumption that the internal rotation rates probed by the seismic splittings are similar to the surface rotation, which appears to be reasonably valid for moderately slowly rotating main-sequence stars, where the splittings are most sensitive to the rotation in the envelope.

The asteroseismic technique provides a useful complement to other existing methods. Observations of the Rossiter-McLaughlin (RM) effect and use of spot-crossing events during exoplanet transits have provided estimates of the sky-projected angle between the planetary orbital axis and the stellar rotation axis in more than 50 systems (Albrecht et al. 2012). The RM observations need bright

targets and are extremely challenging for small planets (e.g. super-Earth-sized objects). Thanks to *Kepler* the spot-crossing method can be extended to much fainter targets (e.g., see Sanchis-Ojeda et al. 2012). However, it also works best on systems with large planets, and on active stars with large spots (to give the required SNR in the spot-crossing events).

In contrast, the asteroseismic method gives information independent of the planet properties, and is therefore useful for investigating alignments in systems with very small planets. However, the limitations of having information on i only must be borne in mind: it is possible for the difference between the orbital and spin angles to be small even when the system is misaligned (e.g., see Hirano et al. 2012). Dependent on the system properties, statistical arguments can however be employed to help discuss the likely correlation of the orbital and spin axes; and the full three-dimensional configuration may of course be recovered when the sky-projected angle and the stellar inclination angle are both available.

Theories which propose that strong misalignments are the result of dynamical interactions (e.g., see Winn et al. 2010) are supported by the well-ordered alignments found in the multi-planet system Kepler-30 studied by Sanchis-Ojeda et al. (2012) using spot-crossing data; and two multiple-systems with solar-type host stars investigated by Chaplin et al. (2013) with asteroseismology. Application of seismology to other *Kepler* systems with RGB hosts, or subgiants showing many mixed modes, will be particularly attractive since the narrow mode peaks are particularly conducive to accurate measurement of the splittings and inclination.

We finish with some remarks on stellar activity and activity cycles. The asteroseismic *Kepler* ensemble offers the prospect of being able to select with high precision and accuracy “evolutionary sequences”, i.e., stars of very similar mass and

chemical composition spanning different evolutionary epochs (Silva Aguirre et al. 2011b), from the main sequence potentially all the way through to the AGB, which may be combined with ground-based observations of stellar activity (e.g. Ca H+K) to give a powerful diagnostic of how activity evolves in solar-type stars, and to better understand the influence that stars have on their local environments (with the obvious implications for exoplanet habitability).

The availability of long timeseries data is now making it possible to “sound” stellar cycles with asteroseismology. The prospects for such studies have been considered in some depth (e.g., see Karoff et al. 2009 and references therein). The first convincing results on stellar-cycle variations of the p-mode frequencies of a solar-type star (the *F*-type star HD 49933) were reported by García et al. (2010), from observations made by CoRoT. This result is important for two reasons: first, the obvious one of demonstrating the feasibility of such studies; and second, the period of the stellar cycle was evidently significantly shorter than the 11-yr period of the Sun (probably between 1 and 2 yr).

The results on HD 49933 are interesting when set against the paradigm (e.g., see Böhm-Vitense 2007) that stars showing cycle periods divide activity-wise into two groups, with stars in each group displaying a similar number of rotation periods per cycle period. The implication is that stars with short rotation periods – HD 49933 has a surface rotation period of about 3 days – tend to have short cycle periods. If other similar stars show similar short-length cycles, there is the prospect of being able to track asteroseismically two or more complete cycles of such stars with the extended *Kepler* mission. We note that Metcalfe et al. (2010a) recently used chromospheric Ca H & K data to detect a short (1.6 yr) cycle period in another F-type star, the aforementioned exoplanet host ι Hor.

Kepler will also make it possible to detect full swings in activity in stars with cycles having periods up to approximately the length of the solar cycle. Detailed analysis of the *Kepler* asteroseismic ensemble is now underway to search for stellar-cycle signatures. Finally, we should not forget the prospects for detecting seismic signatures of stellar cycles from suitably separated (in time) episodic campaigns on ground-based telescopes.

7 Asteroseismology and stellar populations studies

Undoubtedly one of the highlights of the *Kepler* asteroseismology programme has been the detection of oscillations in giants belonging to the open clusters NGC 6791, NGC 6819 (see Figure 7), and NGC 6811 (which has far fewer detections). An obvious advantage of modelling stars belonging to a supposedly simple population is to work under the assumption that all stars have the same age, initial chemical composition, and lie at essentially the same distance. These strong priors reduce the number of free parameters during modelling, allowing for stringent tests of stellar evolutionary theory.

While the analysis and interpretation of asteroseismic data in cluster members is still in its infancy, several promising results have already emerged. Basu et al. (2011) estimated the age, mass and distance of RGB stars belonging to the old-open clusters NGC 6791 and NGC 6819 through application of a grid-based method (see Section 4.1) using the observed $\langle \Delta\nu_{nl} \rangle$, ν_{\max} , photometrically derived T_{eff} , and metallicities from spectroscopic analyses. Given the assumption of a common age and distance, and provided that systematic uncertainties have been accounted for, this approach leads to very precise and potentially very accurate estimates of the cluster properties. Such estimates may be then compared

against those obtained using different techniques and observational constraints (e.g., isochrone fitting, eclipsing binaries). These comparisons, as discussed in Section 4.1, are crucial to test the methods used to estimate radii, masses, and ages of giants, since those methods are also applied to single field stars belonging to composite populations (see below). Stello et al. (2011b) compared the observed and expected $\langle \Delta\nu_{nl} \rangle$ and ν_{\max} to discriminate between asteroseismic cluster members and likely non-members, while Miglio et al. (2012) estimated the integrated RGB mass loss in NGC6791 by comparing the average masses of stars in the RC and on the RGB. The availability of seismic constraints beyond the average seismic parameters, and eventually the comparison between observed and theoretically predicted frequencies of individual modes, will turn these targets into astrophysical laboratories to test models of the internal structure of giants (see Section 5.2).

Along with studies of simple stellar populations, the detection by CoRoT and *Kepler* of oscillations in thousands of field stars has opened the door to detailed studies of stellar populations belonging to the Milky Way, which can be used to inform models of the Galaxy. The mechanisms of the formation and evolution of the Milky Way are encoded in the kinematics, chemistry, locations and ages of stars. Particularly important observational constraints are relations linking velocity dispersion and metallicity to age in different parts of the Galaxy, as well as spatial gradients of metallicity and key abundance ratios at different ages (e.g., for reviews see Freeman & Bland-Hawthorn 2002, Chiappini 2012). The difficulties associated with estimating distances and, to an even greater extent, ages (Soderblom 2010) of individual field stars has been a major obstacle to discriminating between different scenarios of formation and evolution of the major

components of the Milky Way. In this context, solar-like oscillators represent key tracers of the properties of stellar populations.

Once data from the first CoRoT observational run had been analysed, and solar-like oscillations had been detected in thousands of red giant stars (Hekker et al. 2009), it became clear that the newly available observational constraints would allow novel approaches to the study of Galactic stellar populations. Miglio et al. (2009) presented a first comparison between observed and predicted seismic properties of giants observed in the first CoRoT field, which highlighted the expected signatures of RC stars in both distributions. As discussed in Section 4.1, we may estimate radii and masses for all stars with detected oscillations by combining average and global asteroseismic parameters with estimates of surface temperature.

There are several important reasons why asteroseismic data on red giants offer huge potential for populations studies. First, G and K giants are numerous: They are therefore substantial contributors by number to magnitude-limited surveys of stars, such as CoRoT and *Kepler*. Moreover, the large intrinsic oscillation amplitudes and long oscillation periods mean that oscillations may be detected in faint targets observed in the long-cadence modes of CoRoT and *Kepler* (see Section 3). Second, with asteroseismic data in hand red giants may be used as accurate distance indicators probing regions out to about 10 kpc: As in the case of eclipsing binaries the distance to each red giant may be estimated from the absolute luminosity, which is obtained from the asteroseismically determined radius and T_{eff} . This differs from the approach adopted to exploit pulsational information from classical pulsators, notably Cepheid variables, where the observed pulsation frequency leads to an estimate of the mean density only and

hence additional calibration and assumptions are needed to yield an estimated distance. Giants observed by CoRoT and *Kepler* may be used as distance indicators, mapping regions at different Galactocentric radii and, in the case of *Kepler*, exploring regions where thick-disc and halo giants are expected.

Third, seismic data on RGB stars in principle provide robust ages that probe a wide age range: Once a star has evolved to the RGB its age is determined to a first approximation by the time spent in the core-hydrogen burning phase, which is predominantly a function of mass and metallicity. Hence, the estimated masses of red giants provide important constraints on age. The CoRoT and *Kepler* giants cover a mass range from $\simeq 0.9$ to $\simeq 3 M_{\odot}$, which in turn maps to an age range spanning $\simeq 0.3$ to $\simeq 12$ Gyr, i.e., the entire Galactic history. As a word of caution it is worth remembering that estimation of the ages is inherently model dependent. Systematic uncertainties from predictions of main-sequence lifetimes need to be taken into account.

Consider, for example, the impact on RGB ages of uncertainties in predictions of the size of the central, fully-mixed region in main-sequence stars. We take the example of a model of mass $1.4 M_{\odot}$. The difference between the main-sequence lifetime of a model with and without overshooting² from the core is of the order of 20%. However, once the model reaches the giant phase, this difference is reduced to about 5%. Low-mass models with a larger centrally mixed region experience a significantly shorter subgiant phase, the reason being that they end the main sequence with an isothermal helium core which is closer to the Schönberg-Chandrasekar limit (see Maeder 1975), hence partially offsetting the impact of a

²We assume an extension of the overshooting region equal to $0.2 H_p$, where H_p is the pressure scale height at the boundary of the convective core, as defined by the Schwarzschild criterion.

longer main-sequence lifetime. On the other hand, the effect of core overshooting on the age of RGB stars is more pronounced when the mass of the He core at the end of the main sequence is close to (or even larger than) the Schönberg-Chandrasekar limit (e.g., in the case of higher-mass stars, or in models computed assuming large overshooting parameters).

When considering RC stars, an additional complication in the age determination arises from the rather uncertain mass-loss rates occurring during the RGB phase (e.g., Catelan 2009). In this case the characterisation of populations of giants will benefit greatly from estimation of the period spacings of the observed g modes, which we have seen allows a clear distinction to be made between RGB and RC stars (see Section 5.2).

Kepler is contributing significantly to the characterisation not only of red-giant populations, but has also opened the way for “ensemble asteroseismology” of solar-type stars. The detection of solar-like oscillations in about 500 F and G-type dwarfs allowed Chaplin et al. (2011) to perform a first quantitative comparison between the distributions of observed masses and radii of these stars with predictions from models of synthetic populations in the Galaxy. This first comparison showed intriguing differences in the distribution of mass which will need to be addressed with more detail. This sample of stars should provide a gold standard for the age determination of field dwarfs, and further information on age-metallicity relations albeit out to a more limited distance than the giants, of a few hundreds parsecs from the Sun (Silva Aguirre et al. 2012).

8 Concluding Remarks

We finish by looking ahead, with a few remarks on future possibilities to supplement those made already throughout the review. In the short to medium term, there are exciting prospects for fully exploiting the *Kepler* and CoRoT data. The long *Kepler* datasets provide a unique opportunity to make exquisite tests of stellar interiors physics, to probe the internal rotation and dynamics of evolutionary sequences of low-mass stars, and to elucidate our understanding of stellar activity and stellar dynamos by detecting seismic signatures of stellar cycles and applying diagnostics of the internal dynamics. The sample of asteroseismic planet-hosting stars will increase in size as more data are collected and the analysis of the existing raw *Kepler* data continues to evolve. A significant number of systems with red-giant hosts is likely to be added. This will provide crucial results to address how the dynamics of systems, and planet-star interactions, evolve over time (including engulfment of planets).

There is the potential for combining asteroseismic results from *Kepler* and CoRoT with results from large spectroscopic surveys, e.g., APOGEE (Majewski et al. 2010), HERMES (Barden et al. 2010), and the GAIA ESO Public Spectroscopic Survey (Gilmore et al. 2012) (with CoRoT providing results on red giants in different fields of the Galaxy). Since the asteroseismic data provide a very accurate way to determine surface gravities, they can also play an important rôle in helping to calibrate the spectroscopic analyses. A formal collaboration (APOKASC) has already been established between APOGEE and the *Kepler* Asteroseismic Science Consortium. These collaborations open the possibility to provide strong constraints on age-metallicity and age-velocity relations in different parts of the Milky Way.

With regards to future requirements on the asteroseismic observations, there is an obvious need for oscillations data on solar-type stars in clusters (the open clusters observed by *Kepler* are too faint to yield detections in cool main-sequence stars). Such data would allow further tests of stellar interiors physics in main-sequence and subgiant stars and help to calibrate the age ladder. Long timeseries data are also needed on bright stars in the solar neighbourhood. Photometric observations of bright stars of the type proposed for the ESA and NASA candidate missions PLATO and TESS would provide data for asteroseismology limited by intrinsic stellar noise, not photon counting noise. PLATO and TESS would also observe targets in different fields.

There are also exciting developments to come for ground-based asteroseismology. The Stellar Observations Network Group (SONG) of 1-m telescopes is now being deployed (Grundahl et al. 2011), with one of the main goals being the dedicated study of solar-like oscillators. SONG will provide Doppler velocity data of unprecedented quality on a selection of bright, nearby stars, including data on the lowest-frequency modes not accessible to the photometric observations.

9 Acknowledgements

This review has benefited significantly from numerous and varied discussions with many colleagues. We would in particular like to thank Sarbani Basu, Yvonne Elsworth, Ron Gilliland and Arlette Noels for providing detailed feedback on earlier drafts; and Guy Davies and Günter Houdek for their expert help with figures. The authors acknowledge financial support from the UK Science and Technology Facilities Council (STFC). We also acknowledge use of *Kepler* data for some of the figures. These data were made available through the KASC website,

and we thank R. García who prepared the data for asteroseismic analysis.

References

- Aerts C, Christensen-Dalsgaard J, Kurtz DW. 2010. *Asteroseismology*. Springer Science+Business Media B.V.
- Aizenman M, Smeyers P, Weigert A. 1977. *A&A* 58:41
- Albrecht S, Winn JN, Johnson JA, Howard AW, Marcy GW, et al. 2012. *ApJ* 757:18
- Andersen J, Clausen JV, Nordstrom B. 1990. *ApJ* 363:L33–L36
- Appourchaux T. 2011. In *Asteroseismology*, ed. P Pallé, vol. 23 of *Canary Islands Winter School of Astrophysics*. Cambridge University Press. In the press (arXiv:1103.5352)
- Appourchaux T, Chaplin WJ, García RA, Gruberbauer M, Verner GA, et al. 2012. *A&A* 543:A54
- Appourchaux T, Michel E, Auvergne M, Baglin A, Toutain T, et al. 2008. *A&A* 488:705–714
- Arentoft T, Kjeldsen H, Bedding TR, Bazot M, Christensen-Dalsgaard J, et al. 2008. *ApJ* 687:1180–1190
- Asplund M, Grevesse N, Sauval AJ, Scott P. 2009. *ARA&A* 47:481–522
- Ballot J. 2010. *Astronomische Nachrichten* 331:933
- Ballot J, Appourchaux T, Toutain T, Guittet M. 2008. *A&A* 486:867–875
- Ballot J, García RA, Lambert P. 2006. *MNRAS* 369:1281–1286
- Ballot J, Gizon L, Samadi R, Vauclair G, Benomar O, et al. 2011. *A&A* 530:A97

- Barden SC, Jones DJ, Barnes SI, Heijmans J, Heng A, et al. 2010. In *Society of Photo-Optical Instrumentation Engineers (SPIE) Conference Series*, vol. 7735 of *Society of Photo-Optical Instrumentation Engineers (SPIE) Conference Series*
- Basu S, Antia HM. 2008. *Phys. Rep.* 457:217–283
- Basu S, Chaplin WJ, Elsworth Y. 2010. *ApJ* 710:1596–1609
- Basu S, Christensen-Dalsgaard J, Thompson MJ. 2002. In *Stellar Structure and Habitable Planet Finding*, eds. B Battrick, F Favata, IW Roxburgh, D Galadi, vol. 485 of *ESA Special Publication*
- Basu S, Grundahl F, Stello D, Kallinger T, Hekker S, et al. 2011. *ApJ* 729:L10
- Basu S, Mazumdar A, Antia HM, Demarque P. 2004. *MNRAS* 350:277–286
- Basu S, Verner GA, Chaplin WJ, Elsworth Y. 2012. *ApJ* 746:76
- Batalha NM, Borucki WJ, Bryson ST, Buchhave LA, Caldwell DA, et al. 2011. *ApJ* 729:27
- Baudin F, Barban C, Belkacem K, Hekker S, Morel T, et al. 2011. *A&A* 529:A84
- Bazot M, Bourguignon S, Christensen-Dalsgaard J. 2012. *MNRAS* 427:1847–1866
- Bazot M, Vauclair S, Bouchy F, Santos NC. 2005. *A&A* 440:615–621
- Beck PG, Bedding TR, Mosser B, Stello D, Garcia RA, et al. 2011. *Science* 332:205
- Beck PG, Montalbán J, Kallinger T, De Ridder J, Aerts C, et al. 2012. *Nature* 481:55–57
- Bedding TR. 2011. In *Asteroseismology*, ed. P Pallé, vol. 23 of *Canary Islands Winter School of Astrophysics*. Cambridge University Press. In the press (arXiv:1107.1723)

- Bedding TR, Huber D, Stello D, Elsworth YP, Hekker S, et al. 2010. *ApJ* 713:L176–L181
- Bedding TR, Kjeldsen H, Arentoft T, Bouchy F, Brandbyge J, et al. 2007. *ApJ* 663:1315–1324
- Bedding TR, Mosser B, Huber D, Montalbán J, Beck P, et al. 2011. *Nature* 471:608–611
- Belkacem K, Dupret MA, Baudin F, Appourchaux T, Marques JP, Samadi R. 2012. *A&A* 540:L7
- Belkacem K, Goupil MJ, Dupret MA, Samadi R, Baudin F, et al. 2011. *A&A* 530:A142
- Benomar O, Appourchaux T, Baudin F. 2009. *A&A* 506:15–32
- Benomar O, Bedding TR, Stello D, Deheuvels S, White TR, Christensen-Dalsgaard J. 2012. *ApJ* 745:L33
- Bildsten L, Paxton B, Moore K, Macias PJ. 2012. *ApJ* 744:L6
- Böhm-Vitense E. 2007. *ApJ* 657:486–493
- Borucki WJ, Koch DG, Batalha N, Bryson ST, Rowe J, et al. 2012. *ApJ* 745:120
- Bouchy F, Bazot M, Santos NC, Vauclair S, Sosnowska D. 2005. *A&A* 440:609–614
- Brogaard K, Bruntt H, Grundahl F, Clausen JV, Frandsen S, et al. 2011. *A&A* 525:A2
- Brogaard K, VandenBerg DA, Bruntt H, Grundahl F, Frandsen S, et al. 2012. *A&A* 543:A106
- Brown TM, Christensen-Dalsgaard J, Weibel-Mihalas B, Gilliland RL. 1994. *ApJ* 427:1013–1034

Brown TM, Gilliland RL. 1994. *ARA&A* 32:37–82

Brown TM, Gilliland RL, Noyes RW, Ramsey LW. 1991. *ApJ* 368:599–609

Bruntt H, Bedding TR, Quirion PO, Lo Curto G, Carrier F, et al. 2010. *MNRAS* 405:1907–1923

Carter JA, Agol E, Chaplin WJ, Basu S, Bedding TR, et al. 2012. *Science* 337:556–

Catelan M. 2009. *Ap&SS* 320:261–309

Chaplin WJ, Appourchaux T, Baudin F, Boumier P, Elsworth Y, et al. 2006. *MNRAS* 369:985–996

Chaplin WJ, Appourchaux T, Elsworth Y, García RA, Houdek G, et al. 2010. *ApJ* 713:L169–L175

Chaplin WJ, Houdek G, Elsworth Y, Gough DO, Isaak GR, New R. 2005. *MNRAS* 360:859–868

Chaplin WJ, Kjeldsen H, Christensen-Dalsgaard J, Basu S, Miglio A, et al. 2011. *Science* 332:213–216

Chaplin WJ, Sanchis-Ojeda R, Campante TL, Handberg R, Stello D, et al. 2013. *ApJ* 766:101

Charbonnel C. 2005. In *Cosmic Abundances as Records of Stellar Evolution and Nucleosynthesis*, eds. TG Barnes III, FN Bash, vol. 336 of *Astronomical Society of the Pacific Conference Series*

Charbonnel C, Talon S. 2005. *Science* 309:2189–2191

Chiappini C. 2012. In *Red Giants as Probes of the Structure and Evolution of the Milky Way*, eds. A Miglio, J Montalbán, A Noels

- Christensen-Dalsgaard J. 2002. *Reviews of Modern Physics* 74:1073–1129
- Christensen-Dalsgaard J. 2011. In *Asteroseismology*, ed. P Pallé, vol. 23 of *Canary Islands Winter School of Astrophysics*. Cambridge University Press. In the press (arXiv:1106.5946)
- Christensen-Dalsgaard J, Bedding TR, Kjeldsen H. 1995. *ApJ* 443:L29–L32
- Christensen-Dalsgaard J, Houdek G. 2010. *Ap&SS* 328:51–66
- Christensen-Dalsgaard J, Kjeldsen H, Brown TM, Gilliland RL, Arentoft T, et al. 2010. *ApJ* 713:L164–L168
- Christensen-Dalsgaard J, Thompson MJ. 1997. *MNRAS* 284:527–540
- Christensen-Dalsgaard J, Thompson MJ. 2011. In *IAU Symposium*, eds. NH Brummell, AS Brun, MS Miesch, Y Ponty, vol. 271 of *IAU Symposium*
- Cunha MS, Aerts C, Christensen-Dalsgaard J, Baglin A, Bigot L, et al. 2007. *A&A Rev.* 14:217–360
- Cunha MS, Brandão IM. 2011. *A&A* 529:A10
- Cunha MS, Metcalfe TS. 2007. *ApJ* 666:413–422
- de Meulenaer P, Carrier F, Miglio A, Bedding TR, Campante TL, et al. 2010. *A&A* 523:A54
- De Ridder J, Barban C, Baudin F, Carrier F, Hatzes AP, et al. 2009. *Nature* 459:398–400
- Deheuvels S, García RA, Chaplin WJ, Basu S, Antia HM, et al. 2012. *ApJ* 756:19
- Deheuvels S, Michel E. 2011. *A&A* 535:A91
- Demarque P, Woo JH, Kim YC, Yi SK. 2004. *ApJS* 155:667–674

Dupret MA, Belkacem K, Samadi R, Montalbán J, Moreira O, et al. 2009. *A&A* 506:57–67

Eggenberger P, Meynet G, Maeder A, Miglio A, Montalbán J, et al. 2010. *A&A* 519:A116

Eggenberger P, Montalbán J, Miglio A. 2012. *A&A* 544:L4

Escobar ME, Théado S, Vauclair S, Ballot J, Charpinet S, et al. 2012. *A&A* 543:A96

Freeman K, Bland-Hawthorn J. 2002. *ARA&A* 40:487–537

Gai N, Basu S, Chaplin WJ, Elsworth Y. 2011. *ApJ* 730:63

García RA, Mathur S, Salabert D, Ballot J, Régulo C, et al. 2010. *Science* 329:1032–

Gautschy A, Saio H. 1995. *ARA&A* 33:75–114

Gautschy A, Saio H. 1996. *ARA&A* 34:551–606

Gilliland RL, Brown TM, Christensen-Dalsgaard J, Kjeldsen H, Aerts C, et al. 2010. *PASP* 122:131–143

Gilliland RL, Marcy GW, Rowe JF, Rogers L, Torres G, et al. 2013. *ApJ* 766:40

Gilliland RL, McCullough PR, Nelan EP, Brown TM, Charbonneau D, et al. 2011. *ApJ* 726:2

Gilmore G, Randich S, Asplund M, Binney J, Bonifacio P, et al. 2012. *The Messenger* 147:25–31

Girardi L. 1999. *MNRAS* 308:818–832

Gizon L, Solanki SK. 2003. *ApJ* 589:1009–1019

- Gough DO. 1986. In *Hydrodynamic and Magnetodynamic Problems in the Sun and Stars*, ed. Y Osaki
- Gough DO. 1990. In *Progress of Seismology of the Sun and Stars*, eds. Y Osaki, H Shibahashi, vol. 367 of *Lecture Notes in Physics, Berlin Springer Verlag*
- Gough DO, McIntyre ME. 1998. *Nature* 394:755–757
- Gough DO, Thompson MJ. 1990. *MNRAS* 242:25–55
- Goupil MJ, Lebreton Y, Marques JP, Samadi R, Baudin F. 2011. *Journal of Physics Conference Series* 271:012031
- Gruberbauer M, Kallinger T, Weiss WW, Guenther DB. 2009. *A&A* 506:1043–1053
- Grundahl F, Christensen-Dalsgaard J, Gråe Jørgensen U, Frandsen S, Kjeldsen H, Kjærgaard Rasmussen P. 2011. *Journal of Physics Conference Series* 271:012083
- Handberg R, Campante TL. 2011. *A&A* 527:A56
- Hekker S, Debosscher J, Huber D, Hidas MG, De Ridder J, et al. 2010. *ApJ* 713:L187–L191
- Hekker S, Elsworth Y, De Ridder J, Mosser B, García RA, et al. 2011a. *A&A* 525:A131
- Hekker S, Gilliland RL, Elsworth Y, Chaplin WJ, De Ridder J, et al. 2011b. *MNRAS* 414:2594–2601
- Hekker S, Kallinger T, Baudin F, De Ridder J, Barban C, et al. 2009. *A&A* 506:465–469
- Hirano T, Sanchis-Ojeda R, Takeda Y, Narita N, Winn JN, et al. 2012. *ApJ* 756:66

Hole KT, Geller AM, Mathieu RD, Platais I, Meibom S, Latham DW. 2009. *AJ* 138:159–168

Houdek G. 2010. *Ap&SS* 328:237–244

Houdek G, Balmforth NJ, Christensen-Dalsgaard J, Gough DO. 1999. *A&A* 351:582–596

Houdek G, Gough DO. 2007. *MNRAS* 375:861–880

Houdek G, Gough DO. 2011. *MNRAS* 418:1217–1230

Howe R. 2009. *Living Reviews in Solar Physics* 6:1

Howell SB, Rowe JF, Bryson ST, Quinn SN, Marcy GW, et al. 2012. *ApJ* 746:123

Huber D, Bedding TR, Arentoft T, Gruberbauer M, Guenther DB, et al. 2011a. *ApJ* 731:94

Huber D, Bedding TR, Stello D, Hekker S, Mathur S, et al. 2011b. *ApJ* 743:143

Huber D, Bedding TR, Stello D, Mosser B, Mathur S, et al. 2010. *ApJ* 723:1607–1617

Huber D, Chaplin WJ, Christensen-Dalsgaard J, Gilliland RL, Kjeldsen H, et al. 2013. *ApJ* 767:127

Huber D, Ireland MJ, Bedding TR, Brandão IM, Piau L, et al. 2012. *ApJ* 760:32

Kalirai JS, Tosi M. 2004. *MNRAS* 351:649–662

Kallinger T, Mosser B, Hekker S, Huber D, Stello D, et al. 2010. *A&A* 522:A1

Karoff C, Metcalfe TS, Chaplin WJ, Elsworth Y, Kjeldsen H, et al. 2009. *MNRAS* 399:914–923

Kjeldsen H, Bedding TR. 1995. *A&A* 293:87–106

- Kjeldsen H, Bedding TR, Arentoft T, Butler RP, Dall TH, et al. 2008. *ApJ* 682:1370–1375
- Kjeldsen H, Bedding TR, Christensen-Dalsgaard J. 2008. *ApJ* 683:L175–L178
- Kjeldsen H, Bedding TR, Viskum M, Frandsen S. 1995. *AJ* 109:1313–1319
- Kjeldsen H, Christensen-Dalsgaard J, Handberg R, Brown TM, Gilliland RL, et al. 2010. *Astronomische Nachrichten* 331:966
- Lebreton Y, Montalbán J. 2009. In *IAU Symposium*, eds. EE Mamajek, DR Soderblom, RFG Wyse, vol. 258 of *IAU Symposium*
- Lebreton Y, Montalbán J. 2010. *Ap&SS* 328:29–38
- Lebreton Y, Montalbán J, Christensen-Dalsgaard J, Roxburgh IW, Weiss A. 2008. *Ap&SS* 316:187–213
- Maeder A. 1975. *A&A* 43:61–69
- Maeder A, Meynet G. 2000. *ARA&A* 38:143–190
- Majewski SR, Wilson JC, Hearty F, Schiavon RR, Skrutskie MF. 2010. In *IAU Symposium*, eds. K Cunha, M Spite, B Barbuy, vol. 265 of *IAU Symposium*
- Mathis S. 2009. *A&A* 506:811–828
- Mathis S, Palacios A, Zahn JP. 2004. *A&A* 425:243–247
- Mathur S, Metcalfe TS, Woitaszek M, Bruntt H, Verner GA, et al. 2012. *ApJ* 749:152
- Mazumdar A. 2005. *A&A* 441:1079–1086
- Mazumdar A, Basu S, Collier BL, Demarque P. 2006. *MNRAS* 372:949–958
- Mazumdar A, Michel E, Antia HM, Deheuvels S. 2012a. *A&A* 540:A31

- Mazumdar A, Monteiro MJPG, Ballot J, Antia HM, Basu S, et al. 2012b. *Astronomische Nachrichten* 333:1040–1043
- Metcalf TS, Basu S, Henry TJ, Soderblom DR, Judge PG, et al. 2010a. *ApJ* 723:L213–L217
- Metcalf TS, Chaplin WJ, Appourchaux T, García RA, Basu S, et al. 2012. *ApJ* 748:L10
- Metcalf TS, Monteiro MJPG, Thompson MJ, Molenda-Żakowicz J, Appourchaux T, et al. 2010b. *ApJ* 723:1583–1598
- Michel E, Baglin A. 2012. In *Second CoRoT Symposium: Transiting planets, vibrating stars and their connection*, eds. A Baglin, M Deleuil, E Michel, C Moutou. In the press (arXiv:1202.1422)
- Michel E, Baglin A, Auvergne M, Catala C, Samadi R, et al. 2008. *Science* 322:558–
- Miglio A. 2012. In *Red Giants as Probes of the Structure and Evolution of the Milky Way*, eds. A Miglio, J Montalbán, A Noels, ApSS Proceedings
- Miglio A, Brogaard K, Stello D, Chaplin WJ, D’Antona F, et al. 2012. *MNRAS* 419:2077–2088
- Miglio A, Montalbán J, Baudin F, Eggenberger P, Noels A, et al. 2009. *A&A* 503:L21–L24
- Miglio A, Montalbán J, Carrier F, De Ridder J, Mosser B, et al. 2010. *A&A* 520:L6
- Miglio A, Montalbán J, Maceroni C. 2007. *MNRAS* 377:373–382
- Montalbán J, Miglio A, Noels A, Dupret MA, Scuflaire R, Ventura P. 2013. *ApJ* 766:118

- Montalbán J, Miglio A, Noels A, Scuflaire R, Ventura P. 2010. *ApJ* 721:L182–L188
- Monteiro MJPGF. 2009. *Evolution and Seismic Tools for Stellar Astrophysics*. Springer
- Monteiro MJPGF, Christensen-Dalsgaard J, Thompson MJ. 2000. *MNRAS* 316:165–172
- Monteiro MJPGF, Thompson MJ. 2005. *MNRAS* 361:1187–1196
- Mosser B, Barban C, Montalbán J, Beck PG, Miglio A, et al. 2011a. *A&A* 532:A86
- Mosser B, Belkacem K, Goupil MJ, Michel E, Elsworth Y, et al. 2011b. *A&A* 525:L9
- Mosser B, Elsworth Y, Hekker S, Huber D, Kallinger T, et al. 2012a. *A&A* 537:A30
- Mosser B, Goupil MJ, Belkacem K, Marques JP, Beck PG, et al. 2012b. *A&A* 548:A10
- Mosser B, Goupil MJ, Belkacem K, Michel E, Stello D, et al. 2012c. *A&A* 540:A143
- Mosser B, Michel E, Belkacem K, Goupil MJ, Baglin A, et al. 2013. *A&A* 550:A126
- Noels A, Montalbán J, Miglio A, Godart M, Ventura P. 2010. *Ap&SS* 328:227–236
- Ossendrijver M. 2003. *A&A Rev.* 11:287–367
- Palacios A. 2012. In *Red Giants as Probes of the Structure and Evolution of the Milky Way*, eds. A Miglio, J Montalbán, A Noels

- Pinsonneault M. 1997. *ARA&A* 35:557–605
- Pinsonneault MH, Kawaler SD, Sofia S, Demarque P. 1989. *ApJ* 338:424–452
- Popielski BL, Dziembowski WA. 2005. *Acta Astronomica* 55:177–193
- Quirion PO, Christensen-Dalsgaard J, Arentoft T. 2010. *ApJ* 725:2176–2189
- Reese D, Lignières F, Rieutord M. 2006. *A&A* 455:621–637
- Ribas I, Jordi C, Giménez A. 2000. *MNRAS* 318:L55–L59
- Roxburgh IW. 2009. *A&A* 493:185–191
- Roxburgh IW. 2010. *Ap&SS* 328:3–11
- Roxburgh IW, Vorontsov SV. 1997. *MNRAS* 292:L33–L36
- Roxburgh IW, Vorontsov SV. 2003. *A&A* 411:215–220
- Salaris M. 2012. In *Red Giants as Probes of the Structure and Evolution of the Milky Way*, eds. A Miglio, J Montalbán, A Noels
- Samadi R, Belkacem K, Dupret MA, Ludwig HG, Baudin F, et al. 2012. *A&A* 543:A120
- Samadi R, Georgobiani D, Trampedach R, Goupil MJ, Stein RF, Nordlund Å. 2007. *A&A* 463:297–308
- Samadi R, Goupil MJ. 2001. *A&A* 370:136–146
- Sanchis-Ojeda R, Fabrycky DC, Winn JN, Barclay T, Clarke BD, et al. 2012. *Nature* 487:449–453
- Sandquist EL, Mathieu RD, Brogaard K, Meibom S, Geller AM, et al. 2013. *ApJ* 762:58
- Silva Aguirre V, Ballot J, Serenelli AM, Weiss A. 2011a. *A&A* 529:A63

Silva Aguirre V, Casagrande L, Basu S, Campante TL, Chaplin WJ, et al. 2012.

ApJ 757:99

Silva Aguirre V, Chaplin WJ, Ballot J, Basu S, Bedding TR, et al. 2011b. ApJ

740:L2

Smiljanic R, Gauderon R, North P, Barbuy B, Charbonnel C, Mowlavi N. 2009.

A&A 502:267–282

Soderblom DR. 2010. *Annual Review of A&A* 48:581–629

Soriano M, Vauclair S. 2010. A&A 513:A49

Southworth J. 2011. MNRAS 417:2166–2196

Stello D, Chaplin WJ, Bruntt H, Creevey OL, García-Hernández A, et al. 2009.

ApJ 700:1589–1602

Stello D, Huber D, Kallinger T, Basu S, Mosser B, et al. 2011a. ApJ 737:L10

Stello D, Meibom S, Gilliland RL, Grundahl F, Hekker S, et al. 2011b. ApJ

739:13

Straniero O, Domínguez I, Imbriani G, Piersanti L. 2003. ApJ 583:878–884

Talon S, Charbonnel C. 2005. A&A 440:981–994

Tassoul M. 1980. ApJS 43:469–490

Thompson MJ, Christensen-Dalsgaard J, Miesch MS, Toomre J. 2003. ARA&A

41:599–643

Torres G, Andersen J, Giménez A. 2010. A&A Rev. 18:67–126

Torres G, Fischer DA, Sozzetti A, Buchhave LA, Winn JN, et al. 2012. ApJ

757:161

Ulrich RK. 1986. ApJ 306:L37–L40

Unno W, Osaki Y, Ando H, Saio H, Shibahashi H. 1989. *Nonradial oscillations of stars*. Nonradial oscillations of stars, Tokyo: University of Tokyo Press, 1989, 2nd ed.

VandenBerg DA, Bergbusch PA, Dowler PD. 2006. *ApJS* 162:375–387

VandenBerg DA, Stetson PB. 2004. *PASP* 116:997–1011

Vauclair S, Laymand M, Bouchy F, Vauclair G, Hui Bon Hoa A, et al. 2008. *A&A* 482:L5–L8

Ventura P, D’Antona F, Mazzitelli I. 2008. *Ap&SS* 316:93–98

Ventura P, Zepieri A, Mazzitelli I, D’Antona F. 1998. *A&A* 334:953–968

Verner GA, Elsworth Y, Chaplin WJ, Campante TL, Corsaro E, et al. 2011. *MNRAS* 415:3539–3551

Vorontsov SV. 1988. In *Advances in Helio- and Asteroseismology*, eds. J Christensen-Dalsgaard, S Frandsen, vol. 123 of *IAU Symposium*

Weiss A. 2012. In *Red Giants as Probes of the Structure and Evolution of the Milky Way*, eds. A Miglio, J Montalbán, A Noels

White TR, Bedding TR, Gruberbauer M, Benomar O, Stello D, et al. 2012. *ApJ* 751:L36

White TR, Bedding TR, Stello D, Christensen-Dalsgaard J, Huber D, Kjeldsen H. 2011. *ApJ* 743:161

Winn JN, Fabrycky D, Albrecht S, Johnson JA. 2010. *ApJ* 718:L145–L149

Young PA, Knierman KA, Rigby JR, Arnett D. 2003. *ApJ* 595:1114–1123

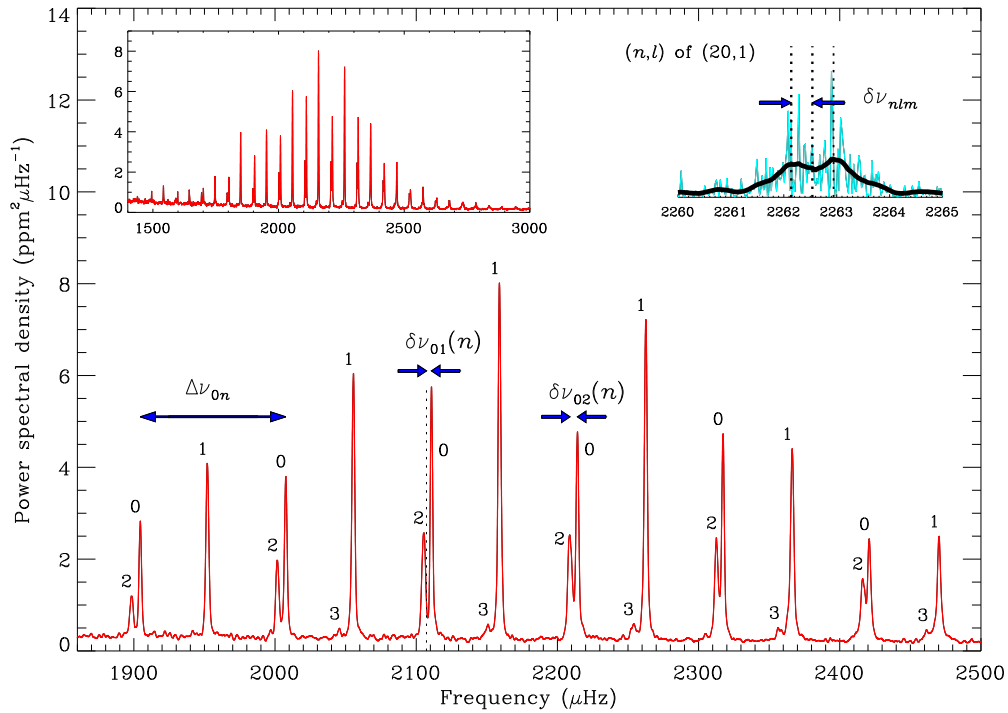


Figure 1: Oscillation spectrum of the G-type main-sequence star in 16 Cyg A (KIC 12069424, HD 186408), as observed by *Kepler*. Main plot: smoothed frequency-power spectrum showing the frequency range containing the most prominent modes in the spectrum, with annotations marking key frequency separations. (The smoothing filter was a double-boxcar filter of width $0.2 \mu\text{Hz}$.) Top left-hand inset: Plot of a wider range in frequency, showing the Gaussian-like modulation (in frequency) of the observed powers of the modes. The frequency of maximum oscillations power, ν_{max} , lies at about $2200 \mu\text{Hz}$. Top right-hand inset: zoom in frequency showing rotational frequency splitting of the non-radial $l = 1$, $n = 20$ mode. The raw spectrum is shown in light blue, and the smoothed spectrum in black. The rotation axis of the star is inclined such that the outer $|m| = 1$ components are visible (outer vertical dashed lines), but the inner $m = 0$ component is not as prominent (central vertical dashed line).

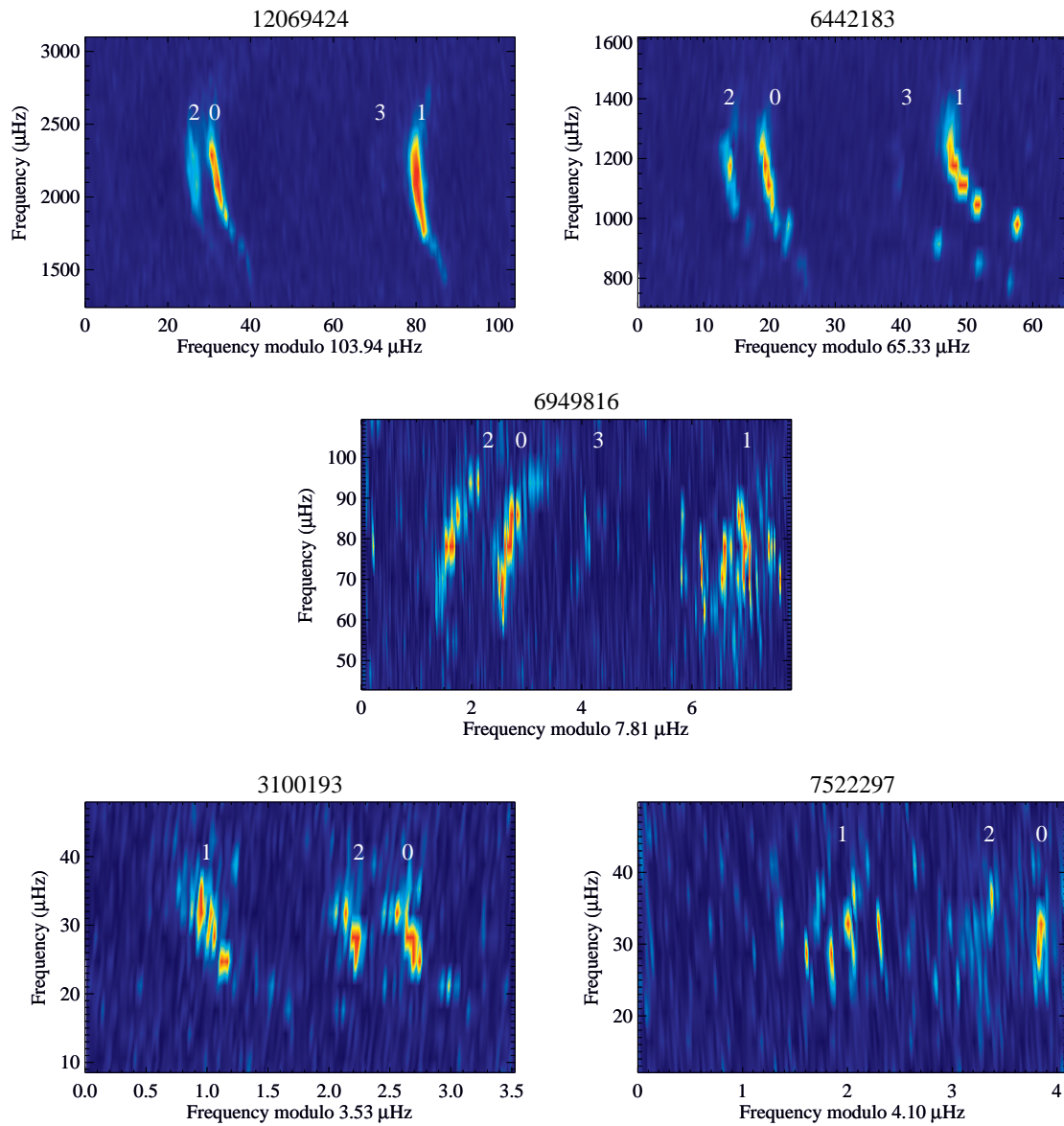


Figure 2: Echelle diagrams (see text) of the oscillation spectra of five stars observed by *Kepler*. Annotations mark the angular degrees, l . Top left-hand panel: diagram for the main-sequence star 16 Cyg A, showing vertically aligned ridges of oscillation power. Note the faint (but significant) power of the $l = 3$ ridge. Top right-hand panel: diagram for the subgiant KIC 6442183 showing a beautiful avoided crossing of the $l = 1$ modes at a frequency around $1000 \mu\text{Hz}$. Middle panel: diagram for the first-ascent RGB star KIC 6949816, which shows clusters of closely spaced $l = 1$ mixed modes. Bottom panels: diagrams of RGB (KIC 3100193) and RC (KIC 7522297) stars that have similar surface properties (note the complexity of the $l = 1$ modes in the spectrum of KIC 7522297 compared to KIC 3100193).

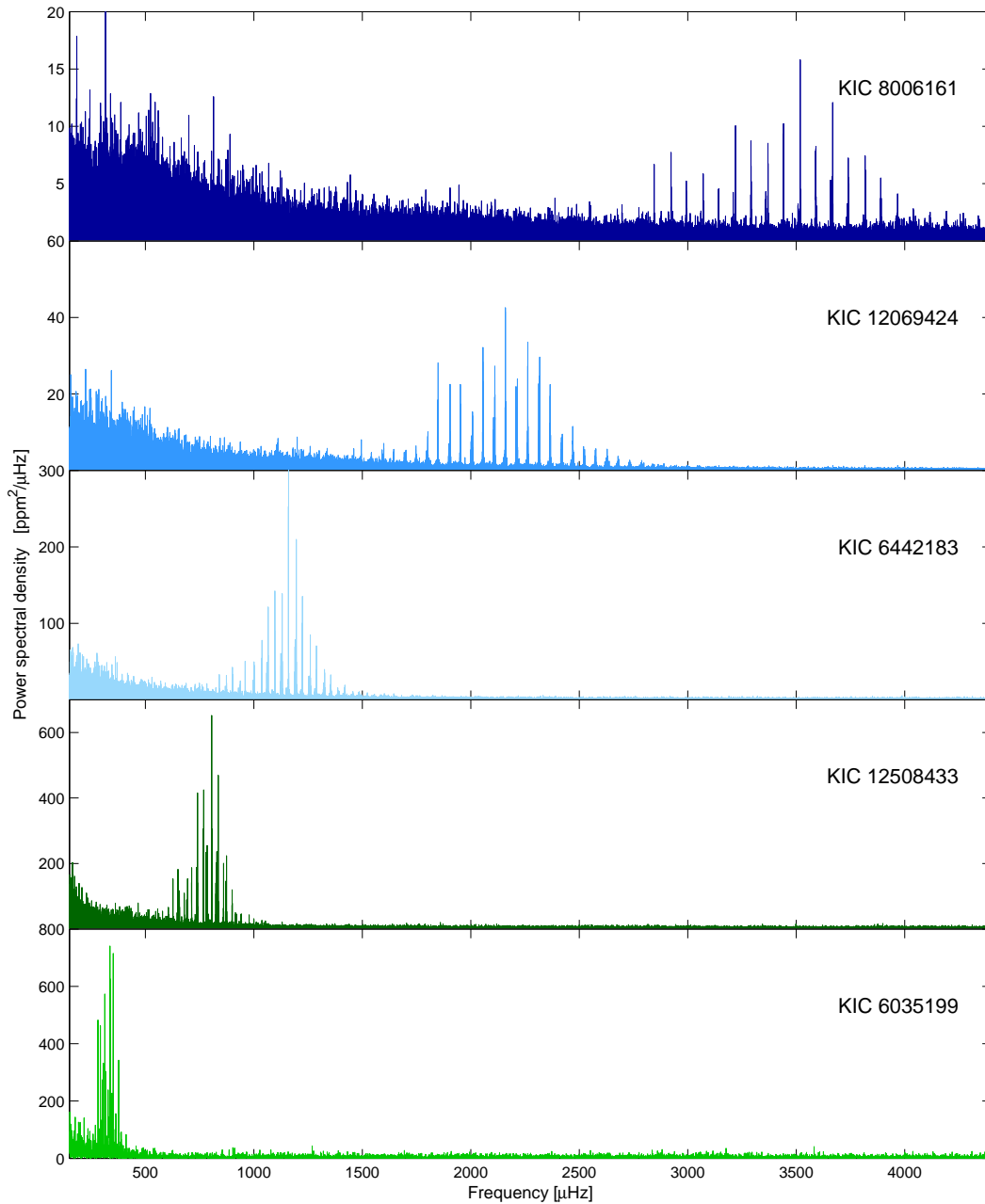


Figure 3: Solar-like oscillation spectra of five stars observed by *Kepler*, using its short-cadence data (see Section 3). Each star has a mass around $1 M_{\odot}$. Stars are arranged from top to bottom in order of decreasing ν_{\max} , i.e., decreasing surface gravity. The top two stars – KIC 8006161 and KIC 12069424 (16 Cyg A) – are main-sequence stars. The third and fourth stars down – KIC 6442183 (HD 183159) and KIC 12508433 – are subgiants. The bottom star (KIC 6035199) lies at the base of the RGB. Echelle diagrams of KIC 12069424 and KIC 6442183 may be found in Figure 2.

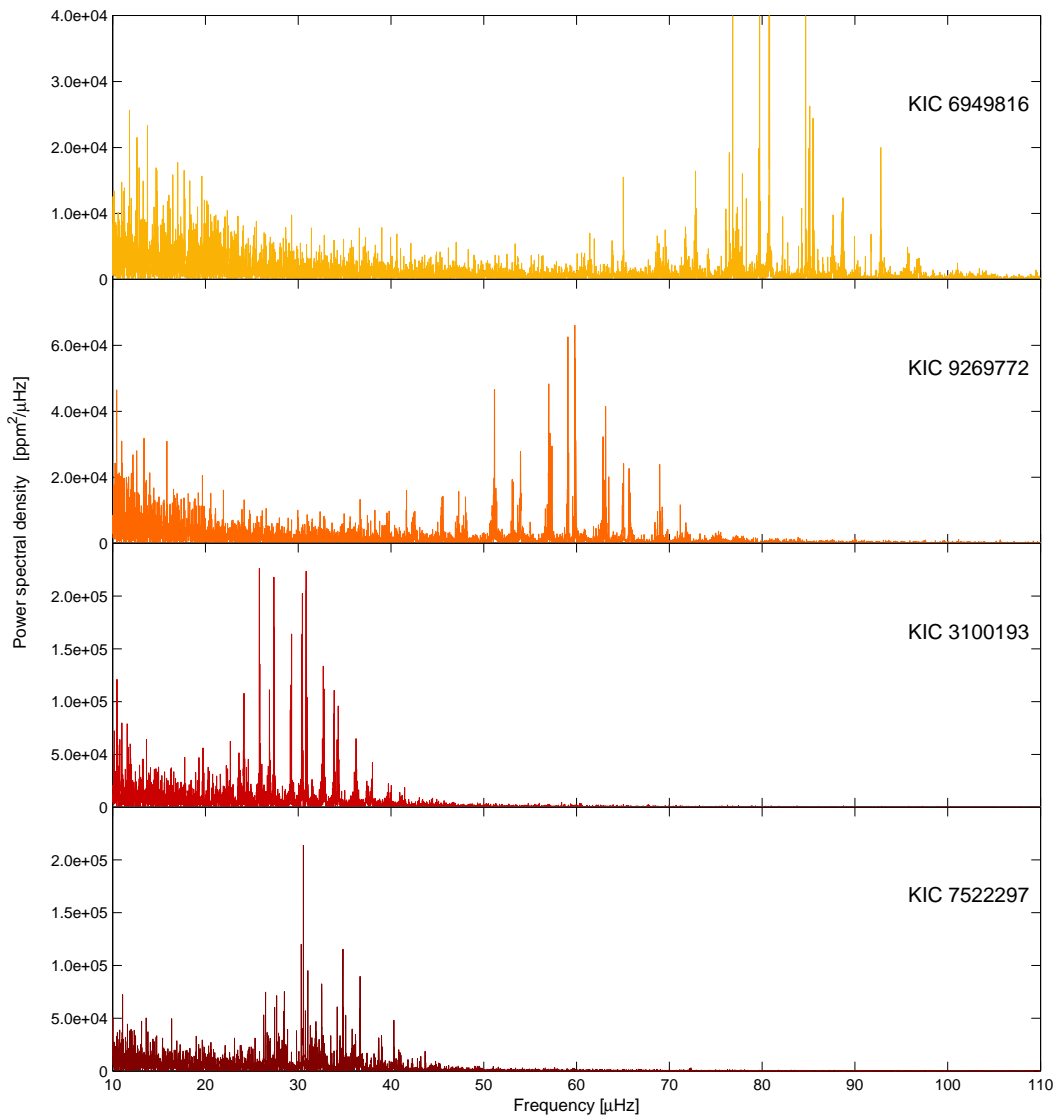


Figure 4: Solar-like oscillation spectra of five stars observed by *Kepler*, using its long-cadence data (see Section 3). Each star has a mass around $1 M_{\odot}$. KIC 6949816 and KIC 9269772 are both first-ascent RGB stars. KIC 3100193 and KIC 7522297 are, respectively, RGB and RC stars sharing similar surface properties. Echelle diagrams of KIC 6949816, KIC 3100193 and KIC 7522297 may be found in Figure 2.

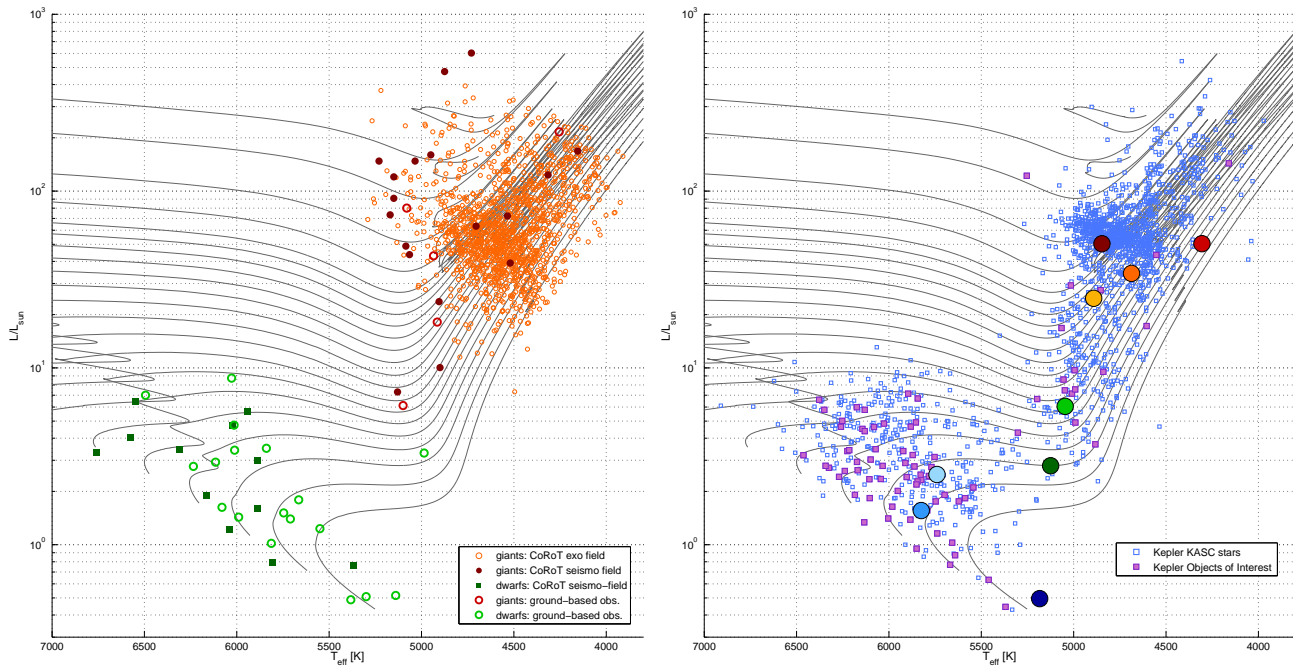


Figure 5: Hertzsprung-Russell diagrams showing populations of stars with detected solar-like oscillations. Left-hand panel: Detections made by CoRoT and ground-based telescopes (see legend). Right-hand panel: Detections made by *Kepler*, including *Kepler* Objects of Interest (see legend). The large coloured circles mark the stars whose spectra are plotted in Figures 1 through 4. Solid lines in both panels follow evolutionary tracks (Ventura, D’Antona & Mazzitelli 2008) computed assuming solar metallicity.

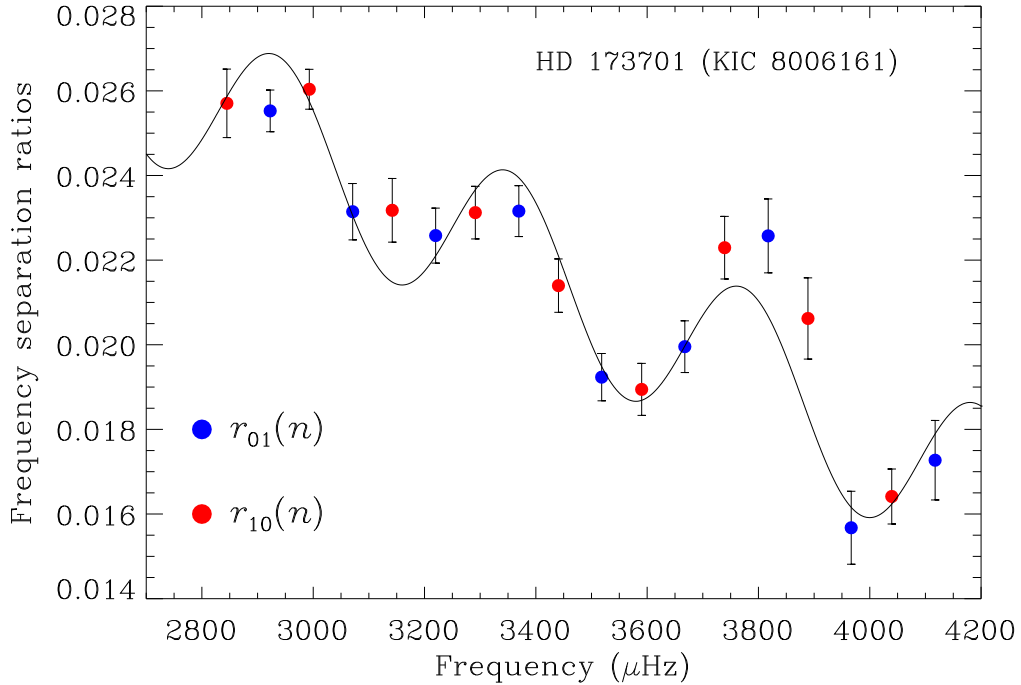


Figure 6: Observed acoustic-glitch signature arising from the base of the convective envelope in the main-sequence *Kepler* target HD 173701 (KIC 8006161; see also Figure 3). The blue [red] points with error bars show frequency separation ratios $r_{01}(n)$ [$r_{10}(n)$] constructed from the estimated $l = 0$ and $l = 1$ frequencies of the star. The black solid line is a best-fitting model (sinusoid plus low-order polynomial) to help guide the eye. The best-fitting period of the sine wave implies that the base of the envelope lies at an acoustic radius of t just under 1200 sec. Given that the acoustic radius of the star is $T_0 \simeq 3350$ s, this implies an acoustic depth τ of approximately 2150 s, i.e., $\tau/T_0 \simeq 0.65$.

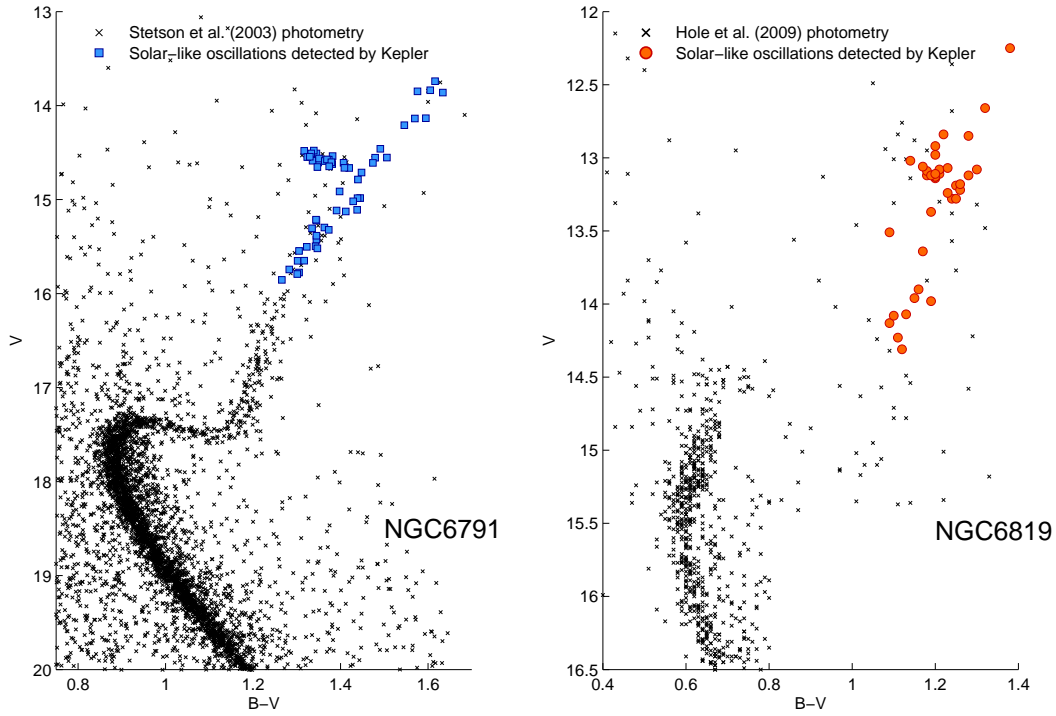


Figure 7: Colour-magnitude diagrams ($B - V$ versus apparent visual magnitude, V) of members of the open clusters NGC 6791 and NGC 6819. Coloured symbols mark the locations of stars with *Kepler* detections of solar-like oscillations (e.g., see Stello et al. 2011b).